HHS Public Access

Author manuscript

Curr Med Chem. Author manuscript; available in PMC 2020 January 01.

Published in final edited form as:

Curr Med Chem. 2019 ; 26(21): 4042–4064. doi:10.2174/0929867325666180226111716.

Organic Fluorescent Dye-based Nanomaterials: Advances in the Rational Design for Imaging and Sensing Applications

Denis Svechkarev[*], **Aaron M. Mohs**[*]

University of Nebraska Medical Center, Department of Pharmaceutical Sciences, Fred and Pamela Buffett Cancer Center, Omaha, United States

Abstract

Self-assembled fluorescent nanomaterials based on small-molecule organic dyes are gaining increasing popularity in imaging and sensing applications over the past decade. This is primarily due to their ability to combine spectral properties tunability and biocompatibility of small molecule organic fluorophores with brightness, chemical and colloidal stability of inorganic materials. Such a unique combination of features comes with rich versatility of dye-based nanomaterials: from aggregates of small molecules to sophisticated core-shell nanoarchitectures involving hyperbranched polymers. Along with the ongoing discovery of new materials and better ways of their synthesis, it is very important to continue systematic studies of fundamental factors that regulate the key properties of fluorescent nanomaterials: their size, polydispersity, colloidal stability, chemical stability, absorption and emission maxima, biocompatibility, and interactions with biological interfaces. In this review, we focus on the systematic description of various types of organic fluorescent nanomaterials, approaches to their synthesis, and ways to optimize and control their characteristics. The discussion is built on examples from reports on recent advances in the design and applications of such materials. Conclusions made from this analysis allow a perspective on future development of fluorescent nanomaterials design for biomedical and related applications.

Keywords

Organic fluorophores; molecular design; structure-property relationship; nanomaterial synthesis; colloidal stability; spectral properties; supramolecular assembly; polymeric aggregates

1. INTRODUCTION

Fluorescence remains one of the most sensitive, powerful and informative sources of data in various domains of chemical analysis and related fields. Along with widespread applications

[*]Address correspondence to this author at the University of Nebraska Medical Center Pharmaceutical Sciences, United States; Tel: 402.559.4336; Fax: 402.559.9543; denis.svechkarev@unmc.edu; aaron.mohs@unmc.edu.

CONFLICT OF INTEREST

The authors declare no conflict of interest, financial or otherwise.

CONSENT FOR PUBLICATION

Not applicable.

of quantum dots - exceptionally bright and stable nanoparticles - major research efforts are focused on development of novel organic fluorescent nanomaterials. Besides being less toxic, nanoparticles composed of organic dyes, often in combination with other components such as polymers or inorganic nuclei/matrices, represent a number of useful properties, including tunability of their spectral properties, potential of being intrinsically responsive to various parameters of their microenvironment and possible multifunctionality, to name a few examples.

The main complexity of designing effective organic dye-based nanomaterials is that fluorescent molecules usually do not perform well even in highly concentrated solutions, and much less in aggregates. Due to reabsorption, energy transfer and other processes they are prone to self-quenching - an effect often referred to as *aggregation-caused quenching (ACQ)*. Research in organic fluorescent nanomaterials experienced a rapid growth in the middle of 2000s (Fig. 1), with the discovery and further development of knowledge about *aggregation-induced emission (AIE)* [1]. As was shown by Tang *et al.*, some molecules demonstrate a quite unconventional feature: they usually exhibit exceptionally weak emission in solutions, but possess rather bright fluorescence in solid state and/or in aggregates. This opened a wide range of possibilities for development of highly effective bright fluorescent nanomaterials based on organic dyes.

Research achievements of the past decade were thoroughly summarized and analyzed in detail in several recent reviews, highlighting current state of the art in synthetic approaches for the preparation of fluorescent nanoparticles [2], applications of nanomaterials for fluorescent sensing and imaging [3], and recent advances in the application of aggregation-induced emission effects for nanomaterials based on carbohydrate polymers [4]. Significant attention has been focused on the development of polymeric structures for biomedical imaging [5,6], in particular in the context of leveraging the power of fluorescence for contrast enhancement in surgery and consequent improvement of cancer surgery outcomes [7]. Nanoparticle probes were also subject of active investigations as perspective agents for fluorescent detection of cancer biomarkers and cells [8].

In the present review, we offer a perspective on recent advances in the development of new fluorescent nanomaterials based on organic dyes. We explore the roles and significance of various structural features and particularities of synthetic processes for design of materials with desired set of properties. Each topic is reviewed in order of increasing complexity: from small molecule aggregates to complex supramolecular structures; from analysis of ions and small molecules to biosensing of microorganisms and multifunctional applications; and from tuning spectral properties to taking control over intermolecular and interparticle interactions for improving colloidal stability. We conclude with an outlook on further research directions that will help advance knowledge and develop better nanomaterials for a wider spectrum of applications.

2. NAVIGATING THE ABUNDANCE

Depending on their composition, organic dye-based fluorescent nanomaterials come in various types that can be represented as a hierarchy stemming from small-molecule

aggregates to complex polymer-based nanoparticles or inorganic-organic nanocomposites. With every type of nanomaterials, its design is aimed to maximize the use of available effects, such as hydrophobic and electrostatic interactions, AIE, anti-ACQ, spectral shifts, etc to obtain optimal properties for intended applications. We hereby discuss the main types of organic and composite nanomaterials employing highly effective fluorophores and AIEgens (such as perylene diimide [9,10], fumaronitrile [11], carbazole [12], triphenylamine [13,14], and tetraphenylethene [15,16]) to achieve bright and stable emission, and a multitude of oligomeric and polymeric materials to improve solubility, colloidal stability and biocompatibility of the resulting nanoparticles.

2.1. Small-molecule Dye Based Self-assembled NPs

Small molecules, upon non-covalent interaction, can produce supramolecular structures of various shapes and sizes. Dye nanoaggregates, the nanostructures presenting the lowest level of organization, are the result of random association of the molecules attracted to each other by hydrophobic, **π-π** or electrostatic interactions. However simple their preparation, such colloidal systems are oftentimes quite irregular in shape and, consequently, rather polydisperse, and show relatively low colloidal stability.

The most straightforward and largely used method of synthesis of organic nanoaggregates is solvent exchange, often referred to as reprecipitation or nanoprecipitation. A solution of the organic dye, having very limited solubility in water, is first prepared in an organic solvent that is miscible with water (tetrahydrofuran and 1,4-dioxane are most commonly used as they are volatile and thus easy to remove, but acetonitrile, acetone, methanol/ethanol or DMSO are also sometimes used) [17]. A small volume of this solution is then injected into water, thus dispersing the insoluble dye as a suspension in a larger volume. This procedure can be also performed with sonication, which may positively influence the dispersion process [18,19].

Among the fluorescent aggregates obtained through solvent exchange, most exhibit AIE properties. A recently reported fluorine-based dye bearing two tetra-phenylethylene (TPE) motifs, for example, demonstrates a remarkable 120-fold increase of fluorescence efficiency upon solvent exchange from methanol to water [20]. Combined with low toxicity, such aggregates are promising for cellular imaging. Interestingly, further fluorescence enhancement was observed upon addition of adenosine triphosphate (ATP), which is ascribed to additional charge-driven aggregation of the cationic dye in presence of phosphate anions of ATP. Aggregates that are obtained through nanoprecipitation are explored not only as prospective imaging agents, but also as materials with dual applications. Thus, a highly emissive pyrene core, being combined with salicylic acid, provides an opportunity to deliver the latter, an effective antimicrobial agent, while retaining its original fluorescent properties [21]. The compound, being formulated in the nanoaggregates with the average particle size of less than 100 nm, is able to penetrate into bacterial cells, as described using *P. aeruginosa* as an example. Visible light triggers photocleavage of the ester bond with subsequent release of salicylic acid. Additionally, the pyrene moiety provides imaging capabilities as a visual control of delivery of the antimicrobial agent. Sensing applications of small-molecule dye nanoaggregates go beyond tracking of drug delivery. A series of phenothiazine derivatives

prepared using a one-step coupling method were demonstrated to dramatically change their spectral properties upon deprotonation [22]. This feature is also exhibited by their aggregates, thus providing an opportunity for sensing of the pH of their microenvironment.

Near-infrared (NIR) fluorescent materials are gaining popularity as imaging agents due to their absorption maxima being located within the so-called tissue optical windows, which allows for better imaging depth and reduces the risk of light-induced tissue damage. Various synthetic and formulation approaches are being actively explored to develop new fluorescent materials with emissions in both NIR-I (700–900 nm) and NIR-II (1000–1700 nm) windows [23]. To achieve this, for example, push-pull molecules are often used, like a recently reported anthraquinone-based dye with a diphenylamine donor moiety [24]. In addition to its electronic properties, the di- and triphenylamine units are widely used for their AIEgenic properties. The aggregates of the resulting compound, obtained through reprecipitation from THF, emit bright NIR fluorescence with a quite large Stokes shift. The aggregates are non-toxic, rather stable at various pH and under continuous light exposure, and have been shown to remain in the cells for more than two weeks and through six generations. This makes them promising for longterm cellular imaging and tracking.

Two-photon absorption has become another soughtfor feature of the fluorophores targeted for bioimaging applications, as it allows excitation of a very limited and precisely defined volume of the samples [25]. An example of a nanomaterial exhibiting this feature was described by Amro *et al.* [26] using the triphenylamine fragment as an electron donor. By expanding the conjugated system and using a bithiophene fragment bearing a carbonyl group as an acceptor, the authors were able to obtain orange-emitting nanoaggregates with relatively high brightness and excellent two-photon absorption in the 700–1000 nm range. Borondifluoride curcuminoids are among other organic molecules recently studied as prospective NIR fluorophores, although they show somewhat smaller fluorescence brightness and two-photon cross-sections compared to the previous example [27]. From the materials design perspective, the authors' conclusion about the role of aromatic end groups in controlling a number of parameters of the product compounds and their nanoaggregates (specifically, their sizes and spectral properties) are of particular interest. To render AIE properties to the borondifluoride moiety, Zhang *et al.* coupled it with a diphenylamine fragment, which also serves as an electron donor to promote the intramolecular charge transfer (ICT) [28]. While the dye's solvatochromism shifts its emission into the red part of the spectrum in polar solvents, the nanoaggregates exhibit green fluorescence due to their lower internal polarity. To enhance cellular uptake and increase the biocompatibility, the aggregates were also prepared using a bovine serum albumin matrix.

Ionic self-assembly is another approach for preparing organic dye colloids from molecules bearing a nonzero charge. One of its significant advantages is much greater control over the self-assembly process to produce nanoparticles with more regular structures. For example, non-fluorescent anions can be used to drive self-assembly of cationic cyanine amphiphiles, as described by Shulov *et al.* [29]. The authors show that this approach affords stable fluorescent nanoparticles <10 nm in diameter that are >40-fold brighter than a single dye molecule (Fig. 2). An important extension of charge-driven nanoassembly is the possibility of co-self-assembly process of several different molecules, resulting in mixed

supramolecular architectures. A good illustration of such an approach is the use of three component dyes with fluorescence colors reproducing the RGB scheme: by controlling their proportions during the solution-phase co-assembly, the authors demonstrated the ability to control the emission color of the resulting nanoaggregates, eventually leading to highly fluorescent white-light emitting nanomaterial [30]. Inspired by ionic liquids, a new type of nanomaterials was proposed by Bwambok *et al.* [31]. The authors used NIR organic cationic dyes in combination with anionic surfactants to obtain fluorescent salts in organic phase, followed by solvent-exchange ultrasound-assisted preparation of the nanoaggregates. The results show that the obtained aggregates are uniform, stable both thermally and colloidally, and are readily uptaken by the cells. Interestingly, variation of the counterion hydrophobicity, size, and steric properties leads to changes in properties of obtained aggregates. The authors attribute such changes, in particular, to different packing of the aggregates - for example, the anion structure affects the ratio of H- and J-aggregates present in the obtained nanomaterials, which influences their spectral properties.

When it comes to imaging applications, the ability to target specific parts of the object under study often becomes a priority. To directly address this need, nanoaggregates are prepared from functionalized precursors that contain targeting moieties. However, co-assembly allows obtaining more versatile materials and brings their design onto a higher level of control. By attaching an active group (*e.g.* azide) to the end of the ethylene glycol side of amphiphilic dye oligomers, post-modification of the resulting nanoparticles has been demonstrated [32]. Further, these active surface groups can interact with click-compatible targeting ligands, which dramatically increases the potential for application of such nanoparticles (Fig. 3). The described experiments show that the density of ligands can be readily controlled by varying the ratio of respective amphiphiles during their co-assembly. The authors also discuss the combination of pre- and post-modification approaches as a way to expand the ligand diversity.

2.2. Dye-polymer Composite NPs

In fluorescent nanomaterials design, polymers are increasingly used in combination with small molecule fluorophores to improve solubility, colloidal stability, and enhance their biocompatibility. Even noncovalent co-assembly of organic dyes with polymers used as matrices usually provides noticeable advantages. This was particularly exemplified by encapsulating AIE bis-thienylbenzodithiophene-based organic dyes into Pluronic F127 triblock copolymer, which led to formation of relatively monodisperse nontoxic nanoparticles that emit bright red fluorescence [33]. The results show that nanoparticle emissions are redshifted with respect to the fluorescence of the respective dyes in the bulk THF solutions. The authors discuss this observation as an argument for effective J-aggregate formation. The team further modified the dye by adding a TPE fragment to enhance its AIE functionality, and followed a similar approach using lecithin to stabilize the dye aggregates [34]. Supporting previous findings with their new results, the authors also report an increase of the fluorescence efficiency of the resulting nanoparticles in comparison to the earlier analogs, which suggests improved anti-ACQ properties. The same effect is achieved with Pluronic F127 used to stabilize the nanoparticles [35].

An alternative way to produce dye-polymer composite nanoparticles is to covalently link both components. This approach, often more elaborate than hydrophobic interaction-based non-covalent co-assembly, potentially offers better stability of the nanoconstructs. Various approaches are used to attach fluorophores with polymers, which can be generally divided into two groups: conjugation of a small molecule with a polymeric backbone, or using the small molecules as a base to perform polymerization reaction. The latter approach was used with a TPE derivative as an initiator for the atom transfer radical polymerization, leading to the synthesis of the AIEgenic conjugate with poly(N-isopropylacrylamide), PNIPAM [36]. Being dispersed in water, which is a “bad solvent” for the TPE fragments, they self-assemble through hydrophobic interactions and π-π stacking, giving rise to bright blue fluorescence. The hydrophilic polymer, in its turn, envelops the aggregates and improves their solubility, stability and biocompatibility. Typically for polyaromatic AIEgens, the authors report remarkable photostability of the resulting fluorescent nanoparticles. With PNI-PAM being a well-known temperature-responsive polymer, the authors also discuss the ability to tune the nanoparticles size with temperature, although potential applications to fluorescent imaging are not revealed. Interestingly, the TPE-PNIPAM nanoparticles were shown to be retained by the cells for rather prolonged period of time, with over 40% of the initial fluorescence intensity still measured after 7 passages.

Various polymers used as backbones are excellent substrates to prepare fluorescent materials through their conjugation with small-molecule dyes, and different chemical strategies are used to make this process simple and efficient. New one-pot methods help optimizing the synthetic procedures. They do not require multiple isolation steps, which usually are the main reasons for loss of material and thus lower yields. Long *et al.* have used the mercaptoacetic acid locking imine reaction to conjugate an amine-terminated PEG derivative with an anthracene-based AIE dye under mild conditions, although using inert atmosphere [37]. The authors suggest this one-pot procedure performs better than most multi-step approaches, whereas the actual yield of the final product is not reported. The authors show that the amphiphilic product readily self-assembles into fairly large spherical nanoparticles that exhibit yellow fluorescence with the quantum yield of almost 9%. A similar one-pot strategy was reported by the same team employing a conjugation between the phenylboronic acid and diols [38]. In this case, the authors used a hyperbranched polyester dendrimer Boltorn H40 in conjugation with a phenothiazine-based AIE dye. The synthesis was followed by self-assembly into orange-emitting nearly spherical nanoparticles that showed excellent photostability during 2 hour-long UV irradiation at 365 nm. Other types of branched polymers can be used as basis for dye-conjugated fluorescent nanoarchitectures. Attachment of a TPE core to polyethyleneimine (PEI) through Michael addition [39] is one of a variety of examples where PEI is used. For these blue-emitting nanoparticles, the authors report a fluorescence quantum yield over 25%, which corresponds to high emission efficiency of TPE and its analogs.

Solvent-free reactions can be viewed as a next step in optimization of synthetic procedures on the way to simplify the preparation of the nanoparticles precursor. A solvent- and catalysis-free Kabachnik-Fields reaction procedure was reported to produce a PEI conjugate with an alkylated phenothiazine derivative [40]. The authors also used ultrasonic radiation to decrease the reaction time and make the synthesis more efficient. Although the exact

mechanism of ultrasonic effect on chemical reactions remains unrevealed, many of them are reported to proceed faster or under milder conditions [41,42].

Polymer generation *in situ* can be effectively combined with the dye conjugation and further crosslinking to facilitate formation of the nanoparticle precursors. For example, a one-pot strategy described to obtain bis-cyanophenylethene-substituted phenothiazine-based fluorescent nanoparticles employs the ringopening polymerization of 4,4'-oxydiphthalic anhydride at room temperature in air, with further addition of polylysine as a linker [43]. Similarly, polylysine can be substituted with glucosamine to obtain glycosylated nanoparticles [44]. In both cases, the resulting materials are characterized with low polydispersity, high stability and low toxicity, and emit red fluorescence.

Various intrinsically hydrophilic natural polymers, particularly polysaccharides, are important alternatives to PEG and similar motifs on the way to solubilize and stabilize the nanoparticles, and improve their biocompatibility. Such polymers can be used as coatings for various nanostructures [45,46]. Alternatively, natural polysaccharides can be modified to self-assemble into polymeric nanoparticles. To achieve this, hydrophobic fragments should be conjugated to the polymer backbone, which will then drive self-assembly in aqueous solutions. Additionally, such nanoparticles can entrap hydrophobic small molecules and serve as delivery vehicles for various cargo, such as drugs or contrast agents. For example, an FDA-approved NIR dye indocyanine green has been reported to effectively load into nanoparticles based on hyaluronic acid (HA) that was modified with N-propyl pyrenebutanamide or N-propyl 5-β-cholanamide hydrophobic side fragments [47]. Due to preferential targeting of the CD44 receptor, commonly overexpressed in cancer tissue, such HA-based nanoparticles demonstrated their potential as contrast agents for fluorescence image-guided tumor surgery. This approach was later expanded to include other dyes, as well as perform their covalent conjugation to a wider range of HA-derived polymers with different molecular weights [48,49]. For example, Cy7.5 conjugated to the HA backbone was demonstrated to be hydrophobic enough to drive self-assembly itself. Co-assembly of polymers, similarly to the approach described above for small molecules and their oligomers, also leads to richer versatility of functional nanomaterials. Thus, mixing two conjugates of hydrophobically modified HA - with Cy7.5 and with Gd^{3+}-DTPA complex - in different proportions allows to control the relative intensities of NIR and MRI signals [50] for multimodal imaging applications - preoperative MRI and intraoperative fluorescent cancer detection. The described materials allow detection of NIR signal in tissue phantoms at the depths of over 5 mm (Fig. 4).

Similarly, another dye, IR1061, which exhibits fluorescence in the NIR-II window, was loaded into the PEGylated nanoparticles and further used for *in vivo* imaging [51]. The authors discuss high photostability and efficient emission of the obtained nanoparticles. The same dye was further employed as a core for layer-by-layer assembly of multifunctional nanoparticles with potential for payload delivery [52]. Hyaluronic acid was used as the outermost coating layer to achieve CD44 targeting.

2.3. Fluorescent Polymer-based NPs

The nanomaterial precursors hierarchy comes to polymers consisting entirely of fluorescent monomers. The so-called polymer dots described by Wu *et al.* [53] are based on squaraine and fluorene copolymers and demonstrate large Stokes shifts together with narrow emission bands in the NIR region. Being excited at 405 nm, the polymers exhibit two emission peaks corresponding to fluorene (~420 nm) and squaraine (~700 nm) monomers. The ratio of intensities of the NIR peak to the blue one increases with the increase of the squaraine *vs.* fluorene content in the polymer. Interestingly, however, the quantum yield of the NIR emission dramatically decreases at the same time. The same effect is observed for the resulting Pdots. The intriguing fact is that the NIR emission is observed under UV excitation, even with almost no spectral overlap between the energy donor (polyfluorene) and acceptor (squaraine). The authors explain the observed effect by the energy transfer through exciton diffusion along the polymer backbone. Remarkably, the resulting Pdots demonstrate a twice narrower emission bandwidth compared to the Qdot705, with the average per-particle brightness ~6 times higher than that of Qdot705.

A combination of an electron-rich benzodifuran and electron-deficient fluorinated thieno-thiophene monomers leads to a fluorescent polymer with a relatively strong emission in the NIR-II window [54]. The authors demonstrate tunable emission in the range of 1050–1350 nm, and successful application of the noncovalently PEGylated nanoparticles for *in vitro* and *in vivo* bioimaging.

Similarly to the constructs discussed above that make use of polyethyleneimine as a basis for dye conjugation, it can be also employed as a linker. For example, hydrothermal treatment of starch with polyethyleneimine leads to formation of fairly polydisperse fluorescent NPs [55]. The authors used the same approach to obtain somewhat smaller fluorescent nanoparticles by conjugating polyethyleneimine with sucrose [56] and dopamine with polyethylene glycol methyl ether methacrylate. Mercaptoacetic acid locking imine reaction discussed above was used in the latter case [57]. In all cases the results show that the obtained nanoparticles exhibit fairly bright fluorescence with quantum yields of up to 15%, which is also dependent on the excitation wavelength. However, neither the origin of the nanoparticles emission, nor the mechanism underlying the excitation wavelength dependence, were discussed. The main advantages of this approach are the use of relatively cheap non-toxic precursors and simple eco-friendly preparation procedure. On the other hand, the notable limitation of such materials for further use in biomedical applications is their rather short-wavelength fluorescence. As a branched polymer, PEI has been shown as an efficient base for nanogels synthesis that can be used for drug delivery. Alginate copolymer with hydrophobically modified PEI was shown to readily encapsulate doxorubicin, and the release is dependent on the environment pH and redox nature [58]. The obtained nanogels are also fluorescent, which adds another function of tracking the drug delivery. An interesting observation was made by the authors on the emission intensity dependence on the pH, which may help shedding more light on the fluorescence mechanism of such polymers in the future.

2.4. Dye-decorated Inorganic NPs

Inorganic nanoparticles can also be combined with organic fluorescent dyes to render them emissive properties. Past decade has seen a notable progress in design of dye-decorated noble metal nanoparticles. In particular, gold and silver nanoparticles attracted much attention of researchers leveraging the advantages of the metal-enhanced fluorescence effects [59].

Silica nanoparticles represent another type of materials with clear advantages, such as well-defined structure, high stability and excellent monodispersity. Mesoporous silica has been actively considered as prospective drug carrier [60,61], thus its combination with fluorescent contrast will have another advantage of drug delivery imaging and tracking. In an attempt to construct such a dual-purpose system, a precipitation polymerization technique was described as a facile approach to cross-link the silica nanoshells with fluorescein *via* its co-polymerization with hexachlorocyclo-triphosphazene [62]. The size and structure of the resulting nanoshells can be tuned by changing the ratio of SiO_2 and the co-polymer precursors. The obtained nanoparticles showed high photostability and doxorubicin loading efficiency of over 25% with rather prolonged release period, which also turned out to be pH-dependent.

Nanocrystalline apatites are regarded as promising cargo carriers, especially for various bone dysfunctions, due to their high resorbability. To assemble multifunctional nanoparticles that would combine therapeutic and imaging functions together with targeting ability, platelet-shaped biomimetic carbonated nanoapatites were labeled with fluorescein isothiocyanate and monoclonal antibody through isothermal adsorption [63]. Even such simple non-covalent labeling approach showed remarkable stability: the release studies of both organic molecules demonstrated that 91% of the initial amount of FITC and 89% of the initial amount of the antibody remained adsorbed after 4 days.

Organic dye aggregates, although being the simplest type of fluorescent nanomaterials in terms of preparation, usually represent rather polydisperse and less stable colloidal systems, thus limiting their applications. Small-molecule and oligomer amphiphiles provide better stability and more ways to control the properties of resulting nanoparticles. Polymer-based nanostructures and organic-inorganic architectures open new horizons for multimodal applications involving dual-mode imaging, drug delivery and theranostics. Co-assembly of both small molecule and polymeric amphiphiles allows achieving diversity and build nanoparticles with various functions.

3. APPLICATIONS OF FLUORESCENT NANOPARTICLES

As nanotechnology becomes more integrated into real-world applications, fluorescent nanomaterials development is increasingly focusing on searching better solutions, particularly, for sensing and bioimaging [64]. Results obtained by researchers over past years has led to formulation of desired characteristics, general requirements and limitations for a variety of materials applied for biomedical imaging [65]. Discussed below are illustrative examples of successful design solutions of supramolecular architectures for imaging and sensing of increasingly complex analytes of biological relevance.

3.1. Biomedical Imaging

Paramagnetic iron oxide nanoparticles, widely investigated as MRI contrasts, can be readily combined with fluorescent motifs to obtain dual-mode imaging agents. For example, high-density core-shell magneto-fluorescent nanoassemblies were prepared by nanoprecipitation [66] in two steps, by first generating the superparamagnetic iron oxide nanoparticles (SPIONs), followed by their *in situ* co-assembly with hydrophobic AIEgenic fluorescent dye to obtain the initial magnetofluorescent platform. On the second step, the latter was coated with various polyelectrolytes to solubilize and stabilize the colloids. This approach allowed to independently study the effect of polyelectrolyte coating on colloidal stability, revealing that long polyanionic chains or block-copolymers are ineffective due to interparticle bridging. In contrast, comb-like PMMA-based polyelectrolites made of relatively short main chains led to excellent stable colloidal systems. The obtained nanoparticles were successfully used for fluorescent and MRI imaging of cells. Using the same FON@mag magnetofluorescent platform, the authors also discussed the role of the stabilizing agents on the performance of the resulting nanoparticles after their internalization into cells [67]. The experiments show that the citrate-coated nanoparticles partially dissociate after crossing the cell membrane, whereas their polyacrylic-coated analogs remain intact after being endocytosed. In general, the magnetofluorescent architecture described above was reported to exhibit very insignificant fluorescence quenching by the iron oxide inclusions. Such morphology also improves the MRI contrast by creating an inhomogenous magnetic field via dispersion of small. SPION particles within the hydrophobic fluorescent core.

Fluorescent nanoparticles linked to targeting ligands become able to selectively image tissues, cells or subcellular features of interest. In a simple example, the pyrene fluorophore, well-known for its exceptional brightness and photostability, was conjugated to biologically active guanine analogs. Their aggregation in water led to a pronounced bathochromic shift and quenching of the observed emission. Interesting experiments were performed on isolated model fragments of one of the conjugates to evaluate their concentration-dependent spectral behavior and reveal their roles in the aggregation process. Results showed that the pyrene fragments play the key role in aggregation, most probably through π-π interactions [68]. Imaging capabilities of the obtained nanoparticles were tested with breast cancer cells and zebrafish embryos. In the latter case, zebrafish treated with both nanoparticles showed selective fluorescence of muscle fibers, and presented notable photostability.

Fluorescent motifs can also be used for imaging control of the targeted drug delivery. In the simplest case, the imaging and therapeutic components will be conjugated into single molecule with cleavable linker. An anticancer drug chlorambucil can be particularly conjugated to an acridine derivative through an ester bond that was shown to be photocleavable [69]. Aggregates prepared by reprecipitation from acetone are readily internalized into cells, and preferentially accumulated in the cell nuclei due to specific targeting ability of the acridine fragment. Visible light triggers the cleavage of the ester bond and subsequent release of the drug, which was confirmed *in vitro* by means of HPLC-controlled photolysis experiments and further demonstrated by significant increase of cytotoxicity of the photoresponsive material after irradiation. Another interesting effect has been observed with tetraethyl anthracene-9,10-dyil-9,10-bisphosphonate nanoaggregates

[70]. Beside the imaging capability due to presence of the anthracene fragment, they were shown to be potent as active agents for apoptosis-mediated cancer therapy. The authors show that the precursor molecules self-assemble into 30–40-nm nanoaggregates that specifically exhibit cytotoxicity towards human histocytic lymphoma cancer cells, and showed no particular interaction with other cancer cells.

3.2. Sensing and Theranostics

Sensing of a variety of analytes represents interest in terms of evaluation of mechanisms of biological processes, diagnosing diseases and searching for better treatments. When it comes to design, biologically-relevant ions can be considered among the easiest targets. However, providing relevant selectivity and specificity can be even more challenging than in the case of larger molecules, *e.g.* aminoacids or polypeptides.

There are multiple approaches for ion sensing. One of the recent examples describes a TPE-based nanomaterial that readily co-assembles upon interaction with ATP [71]. The presursor molecule is hydrophilic as the TPE core is attached to two short PEG chains containing imidazolium cations. As the TPE moiety is a well-known AIEgen, the molecule itself displays rather weak fluorescence in solution. Due to its cationic nature, the compound undergoes charge-driven self-assembly with ATP that bears negatively-charged anions. The sizes of resulting nanoaggregates significantly depend on the concentration of ATP. As a consequence, a dramatic increase of fluorescence intensity is observed. The resulting aggregates, offering an abundance of coordination sites, were demonstated to have exceptional selectivity for Fe(III) ions (Fig. 5). The authors suggest that the observed quenching may be caused by iron ions coordination into imidazolium chelation cavities, which brings the former close to the TPE moieties and promotes the energy transfer through the metal center. It is worth noting that the authors carefully considered the possible effect of other anions on the precursor molecule self-assembly, and found that a few of the anions tested induced only a slight increase of emission, whereas more than 7-fold increase was observed in presence of ATP. As a result, the described nanoaggregates are capable of selective Fe(III) sensing with subnanomolar detection limit. Alternatively, the direct interaction of the chelator with the analyte can provide the analytical signal, as described for example in the case of N,N’-propylenebis(salycilimine)-based nanoaggregates sensitive to Al(III) ions content [72]. Another remarkable difference from the iron(III) sensor discussed above is that this probe provides a *turn-on* signal, compared to quenching-based *turn-off* principle mentioned previously. Usually, turn-on sensors are considered as those providing better contrast and higher accuracy of detection. In this case, chelation with Al(III) leads to restriction of intramolecular motions within the molecule and thus results in increase of the emission intensity. The authors demonstrate the application of their nanoaggregate for Al(III) content imaging in *Staphylococcus aureus* and *Salmonella typhi*. Very similar approach was used by the same team to develop a sensor nano-material for Zn(II) ions. The authors used a chelator based on bis-pyridine substituted ethylenediimine that formed nanoaggregates through nanoprecipitation from the THF solution [73]. Due to the presence of four tertiary nitrogens, the molecule readily forms chelate complexes with Zn(II) ions which leads to the increase of the aggregate’s emission intensity, as discussed above. Appropriate competitive binding studies have been performed with other cations and anions,

and no significant interference was detected. The applicability of the obtained nanoaggregates was exemplified by analysis of Zn(II) content in multivitamin formulation samples with the errors less than 5% compared to the reported values. Another example of displacementbased sensing has been reported by Kaur *et al*. [74] using nanoaggregates based on pyrene-substituted derivatives of dihydropyrimidone. One-pot multicomponent Biginelli reaction strategy was used to prepare the precursor fluorescent molecules, and the aggregates were obtained using the reprecipitation method from the dye solution in methanol. Metal complexation properties were studied for all aggregates, and sulfur-containing derivatives were shown to be selectively responsive to Hg(II) ions, in good accordance with the HSAB principle, with one of them exhibiting notable enhancement of the monomer fluorescence upon interaction. Competitive binding studies showed no significant interference from other metal cations and most of anions. However, the presence of iodide anion led to decrease of fluorescence intensity with good linearity with respect to the anion concentration. To demonstrate the potential of the discovered sensor for analysis of real samples, the authors performed analysis of iodide content in tap water, urine and blood serum, which demonstrated high accuracy with subnanomolar detection limit.

Apart from the traditional approach when a reporter is designed to specifically respond to a particular analyte, selectivity can be also achieved by combining non-specific responses from multiple reporters. This approach, often referred to as *chemical nose*, has been gaining much popularity primarily for small molecule sensing. However, in a report by You *at al.* the authors employed non-covalent conjugates of gold nanoparticles (AuNPs) with a fluorescent polymer to demonstrate the performance of this approach for protein identification [75]. Upon interaction with different proteins, six fluorescent polymers, initially quenched by their proximity to the gold nanoparticles, demonstrate various patterns of fluorescence recovery based on their binding affinities to the AuNPs compared to the competing proteins. This way, a unique bar code-like combination of spectral response can be obtained for each protein, providing the identification accuracy of almost 95%. With many advantages of this method, its only notable weakness is the need to control the concentration of the protein samples.

Using highly solvatochromic push-pull chromophores allows tracking the dynamics of the fluorescent nanoparticles upon their interaction with the biological systems. Organic dyes based on diphenylamine and cyanophenylethylene as donor and acceptor, respectively, have been reported to exhibit significant hypsochromic emission shift upon their self-assembly, compared to their orange-red fluorescence in bulk solutions in polar organic solvents [76]. The emission further shifts towards short wavelengths upon the aggregates disassembly and the dye localization into less polar environments. Fluorescent microscopy was used to show that the aggregates are rapidly dissociated by the macrophages, whereas they remain intact longer in the cancer cells. Earlier the same team used a similar dye, but without alkyl substitution, to demonstrate the aggregates dynamics after their cellular uptake, including the initial formation of membrane vesicles enveloping the nanoaggregates, and further release of the dissociated molecules into the cytoplasm [77]. It is noteworthy that the reported dyes exhibit both efficient one- and two-photon excitation. Understanding of the behavior of nanoparticles of different composition and morphology after their uptake into cells is of great importance. The authors of a recent study [78] used a combination of

analytical methods such as electron and fluorescent microscopy, light scattering, FASC, surface-enhanced Raman scattering, *etc.* Experiments were focused on investigating the stability of ATTO590-decorated gold nanoparticles in lysosomes. They conclude that fluorescence-based analytical methods are prone to a number of sources of potential inaccuracies like bleaching, dye leakage and quenching, that may significantly influence the results. In particular, it was shown that stability and integrity of the polymer-grafted nanoparticles with incorporated fluorophores are significantly influenced by the lysosomal environment, leading to their aggregation and loss of fluorescence.

A variety of nanomaterial-based sensors have been described for detection, monitoring and imaging of biogenic thiols. Employing the displacement-based technique, the complex aggregates of a naphthalene derivative with Fe(III) ions was described to have a selective spectral response to 4,5-diamino-6-hydroxy2-mercaptopyrimidine [79]. The most relevant explanation of the emission enhancement upon increasing concentration of the analyte is the decomplexation of Fe(III) ions that can act as quenchers. Interestingly, the same complex aggregate also showed selective response to tyramine, which makes it a multianalyte sensor. The reported detection limits are within the nanomolar concentration range. Another aggregated complex, containing ions of Hg(II) chelated with a rhodamine-based fluorescent dye, was earlier shown to effectively detect 3-mercaptopropionic acid [80]. Competition studies have been performed with a series of anions, biologically relevant thiols and acids, and no significant interference was observed. Similarly to earlier strategies of coupling excited-state proton transfer (ESIPT) cores with highly emissive motifs to obtain bright fluorophores with dual emission [81,8], 2 a hydroxyphenyl-benzthiophene core was combined with the TPE AIEgenic moiety to combine both features in one compound [83]. While in organic solvents the product exhibits dual-band emission, only the phototautomer fluorescence is observed from its aggregates in water. Upon protecting the hydroxyl group, the fluorescence is quenched due to hindrance of ESIPT. Reaction with a thiol allows removing the protective fragment and restores the intramolecular H-bond, giving rise to ESIPT emission (Fig. 6). A multiplex approach using multiple binding site probes has been applied to detect and differentiate between a variety of biogenic thiols [84]. This method not only allows distinguishing between various biothiols (namely cysteine, homocysteine and glutathione), but can also enable their simultaneous monitoring. A more complex approach to imaging the reductive environments in living cells was proposed using Rhodamine B doped silica nanoparticles. They were subsequently coated with Pluronic F127 pre-functionalized with Black Hole Quencher - 2 (BHQ-2) molecules through disulfide linkers. These can be cleaved upon reduction, thus allowing for recovery of fluorescence with the decrease of FRET efficiency [85]. Fluorescence lifetime imaging (FLIM) was demonstrated to be a valuable complementary technique to conventional intensometric measurements.

Charge-driven response was employed for D-penicillinamine sensing. The nanoaggregates were prepared using the reprecipitation method from a bisnaphthalene-2-ol Schiff base derivative and subsequently stabilized with CTAB. The resulting nanomaterial emits yellow fluorescence and bears a positive surface charge due to the nature of the stabilizing surfactant [86]. In expectation of favorable interaction with negatively charged analytes, fluorescence measurements were performed for the nanoaggregates upon interaction with various aminoacids and other biologically-relevant molecules. Parallel competition

measurements were made with metal cations - however, almost no data on possible interference from anions is reported. The aggregates selectively turn off the fluorescence in the presence of D-penicillinamine with rather low detection limit of 0.02 ppm. Dopamine sensing was achieved with TPA-based dye nanoprecipitated with Pluronic F127 [87]. The nanoparticles exhibit strong fluorescence with the maximum around 560 nm. However, the emission is efficiently quenched in the presence of dopamine. To reveal the quenching mechanism, the authors performed experiments with free do-pamine and polydopamine in solution, and concluded that the decrease in fluorescence is due to the charge transfer between the organic dye and the polydopamine layer that envelops the nanoparticles upon the dopamine self-polymerization. Their report contains detailed discussion of the sensing conditions optimization, as well as describe the exemplary analysis of dopamine in blood serum samples.

More complex sensing architectures are being developed not only for sensing of particular properties of the microenvironment or concentrations of a particular analyte, but to enable monitoring of important processes in cells. For example, endosomal escape is of ultimate importance for improving drug efficacy. To achieve this, a PDMA-based block copolymer was designed containing two dyes on its backbone - a pH-sensitive coumarin and pH-insensitive rhodamine [88]. The polymeric nanoparticles were prepared using the solvent exchange method, where the water-DMF polymer-containing solution is dialyzed against water to remove DMF and promote self-assembly. Importantly, the block copolymer is also pH-responsive, allowing the nanoparticles disassembly upon endocytosis. Consequently, the blue emission of coumarin is quenched in the acidic organelles, and only rhodamine’s red emission is detected. As a result of endosomal escape, the polymer enters the cytosol, where coumarin’s emission is restored under near-neutral pH of the environment. Such ratiometric construct enables effective monitoring and mapping of the intracellular pH in a rather wide range (Fig. 7).

Dye-based nanomaterials also enable detection of microorganisms. A pyrimidine-based fluorescent dye aggregates obtained through nanoprecipitation from its solution in DMSO demonstrated selective sensitivity to *Pseudomonas aeruginosa* bacterial species, as reported by Kaur *et al* [89]. Parallel experiments were performed to assess the response of the sensor to the presence of other Gram-positive and Gram-negative microorganisms and even a few fungi, but no notable interference was observed. The sensor was further tested on environmental samples and proved to give very similar results to those obtained with the plate count method. The detection limit was determined at the level of 46 CFU.

As previously mentioned, fluorescent motifs often become part of multifunctional nanomaterials. In particular, their imaging and diagnostic functions can be combined with drug delivery or other therapeutic applications. Similarly to an earlier discussed photoresponsive pyrene-salicylic acid conjugates [21], perylene-based conjugate with chlorambucil forms nanoaggregates that act as delivery vehicles with release tracking ability [90]. The initial nanoaggregates exhibit red fluorescence, and the ester bond between the drug and the fluorophore is cleaved by visible light. Inspired by these promising results, the authors further developed this platform to add another function. They reported creating a nanoparticle based on a branched PEG, which was functionalized with biotin to increase the

specificity of anticancer drug delivery. This intermediate was consequently functionalized with the coumarin-chlorambucil conjugate [91]. While chlorambucil's function is clear, the authors used coumarin not only as an imaging motif, but also as an active agent for photodynamic therapy (PDT, a 37% singlet oxygen quantum yield is reported).

An alternative nanomaterial for PDT applications was proposed by Chang *et al.* [92]. The authors used a dipyridyl-carbazole derivative, BMVC, conjugated to a porphyrin derivative as a photosensitizer. From one to four BMVC fragments were attached to the porphyrin core, and the resulting molecules were self-assembled into red-emitting fluorescent nanoaggregates. Beside its main role as a FRET donor, BMVC also acts as the targeting moiety: the authors describe preferential accumulation of the aggregate in the cancer cells. FRET singlet oxygen generation was dependent on the number of BMVC antennae present in the molecule, while almost no dark toxicity was observed. The authors of a recent report [93] explored the potential of poly(3-hexylthiophene-2,5-diyl), P3HT, a polymer that is largely used in optoelectronic devices, as an agent for PDT. P3HT was mixed with PSMA, an amphiphilic block copolymer, to obtain water-dispersible core particles using the reprecipitation method. A red-emitting fluorescent dye, a derivative of dicyanomethylene-4*H*-pyran, was conjugated with galactose and mannose. The latter acted as targeting moieties for the corresponding receptors in hepathic and breast cancer cells, respectively. The polymeric cores were noncovalently coated with the dye-saccharide conjugates. Selective activity of the obtained PDT agents was demonstrated against hepathic (Hep-G2) and breast (MDA-MB-231) cancer cell lines, and minimal phototoxicity was observed in case of HeLa cells.

Dye-based nanomaterials are applied for a wide spectrum of imaging and sensing applications. This includes detection of important ions, small and large biomolecules, and microorganisms in model systems, biological fluids and other natural samples. Sensing nanomaterials have been developed for analysis of different parameters of their microenvironment, such as pH gradients with subcellular resolution. This provides unique information for further development of our knowledge about fundamental biological processes. Strategies for synthesis of multifunctional nanomaterials, such as co-assembly, present new avenues for creation of materials capable of performing numerous functions, for example, multimodal imaging or theranostics agents. Design of imaging and sensing nanomaterials often relies on conservation of the initial properties of small molecules used. However, smart combination of their individual features can lead to new capabilities at the supramolecular level.

4. PERFORMANCE OPTIMIZATION

Multiple factors combine together to determine a whole spectrum of chemical, colloidal and photophysical properties of fluorescent nanomaterials. In order to efficiently design materials with desired properties, it is thus very important to apply systematic knowledge on structure-properties relationships in small molecule components, as well as their interplay with interactions at supramolecular level [94]. Using various theoretical instruments and synthetic approaches, better solubility, stability, brightness, *etc.* can be achieved for nanomaterials [95].

4.1. Absorption and Emission

Having control over the absorption and emission wavelengths of fluorescent nanomaterials pursues one or more of the three main goals: being able to shift the absorption and emission maxima to develop a palette of colors for simultaneous multicolor imaging; creating nanomaterials with narrow absorption and emission spectra to enable better selectivity in excitation of a particular fluorophore (alternatively - seeking for wide absorption spectra for easier or more effective excitation); and designing new long-wavelength fluorescent materials for NIR imaging that would be free of traditional flaws of the dyes in this spectral range - relatively low quantum yields and photostability.

The most common ways to achieve a bathochromic shift of both absorption and emission for a particular compound is to expand its conjugated system and enhance the intramolecular charge transfer. A systematic demonstration of this approach was described by Genin *et al.* [96], where the authors designed a triarylamine-based push-pull fluorophore with thiobarbituric acid as an electron acceptor and bis-thiophene linker between them. Additionally, bulky *tert*-butyl substituents were introduced to hinder the tight antiparallel packing of the molecules upon aggregation, which is one of the main reasons for low efficiency of emission. While the emission maximum of the dye in bulk solutions varied from 600 to 900 nm, its aggregate in water exhibited fluorescence peaking at 800 nm. Importantly, exceptional brightness was also achieved, indirectly estimated to surpass the typical NIR dyes by several orders of magnitude.

To complement and extend the capabilities beyond the coarse tuning of absorption and emission wavelengths discussed above, an elegant example of fine tuning of spectral properties of organic fluorescent dyes was recently reported using rhodamine derivatives as an example [97]. The authors achieved slight shifts in the absorption and emission in small molecules using inductive electronic effects of substituents. They showed excellent correlation of the observed absorption maxima with both theoretically calculated values, as well as with inductive Hammett constants of the respective substituents, and the observed effects were shown to be additive. In addition, influence of the substituent’s electronic nature was found to influence the lactone-zwitterion equilibrium that regulates the emission efficiency of the chromophore.

Tuning the emission of the fluorescent nanoparticles can be achieved even without changing the spectral properties of the components, as demonstrated with using FRET [98]. The approach is based on doping of the nanoaggregates of 1,4-dimethoxy-2,5-bis(4chlorostyryl) benzene (DCSB) - a blue-emitting dye with a strong two-photon absorption cross-section. Combined with a few commercially available dyes - coumarin 6 (green emission), rubrene (yellow emission) and DCM (orange emission) - the DCSB matrix absorbs the excitation and transfers the energy to the dopants that consequently emit fluorescence of corresponding color. Mixed aggregates with the dopant content of up to 10% were obtained using the modified reprecipitation method. Thus, close proximity of the dyes inside such mixed aggregates ensure high FRET efficiency.

The concept of size-dependent emission wavelength is very well known for quantum dots. Intriguingly, there are examples among the organic fluorescent nanomaterials when particles

of different sizes will have different spectral properties. Thus, controlling the time of the polymerization reaction allows for obtaining polydopamine nanoparticles with tunable emission [99]. The main drawback of polydopamine nanostructures - their polydispersity and relatively low stability - has been overcome by using carbon dots as seeds for dopamine self-polymerization. Upon increase of the polymerization time, a rise of a long-wavelength emission band is observed, causing the apparent bathochromic shift of fluorescence. The authors ascribe the effect to FRET from the carbon dots to polydopamine. Size-dependent emission was also described for a number of pyrazoline derivatives [100].

FRET is only one of the avenues to control the emission characteristics of the nanomaterials through intermolecular interactions inside the supramolecular structure. Formation of molecular aggregates of different types, namely J- and H-aggregates, influences the spectral properties of the resulting nanomaterial. For example, carbocyanine ionic dyes can form salts with various organic anions through ion exchange reaction, and can be further dispersed in water using the reprecipitation method [101]. The results show that various anions can favor formation of either J- or H-aggregates, thus the counterion-controlled J/H ratios is demonstrated to determine the spectral properties of the resulting nanoaggregates.

A different approach can be taken while using organic or inorganic matrices to produce dye-doped nanoparticles. Encapsulating single dyes in such nanocages was reported to prevent them from self-quenching even at high effective concentrations, as each “guest” dye molecule is effectively isolated from the neighbors inside the zeolite-like hydrogen bond framework consisting of tris(guanidinium) nitrate and hexa(4-sulfonatophenyl)benzene fragments [102]. Moreover, the choice of the dyes can serve as a simple way to control the emission color of the obtained nanomaterial.

4.2. Brightness and Chemical Stability

The nature of intermolecular association not only influences the emission maxima, but also plays a vital role in fluorescence efficiency of the dye aggregates. Excessive formation of “dark” excimers can be particularly addressed by preventing antiparallel association through steric hindrance [96]. Alternatively, the shortrange ordering of the ionic rhodamine-based dye aggregates was controlled through the fluorination of the hydrophobic tetraphenylborate counterion [103]. Results showed that gradual fluorination led to decrease in the H-aggregation of the dyes, and resulted in dramatic improvement of the nanoaggregates brightness. The particles obtained using the most fluorinated tetrakis-(3,5-bis-(1,1,1,3,3,3-hexafluoro-2-methoxyisopropyl) phenylborate counterion showed a ~100-fold quantum yield improvement compared with those co-assembled with tetraphenylborate. A systematic study was performed to explore the interplay between the aggregation-caused quenching (ACQ) and aggregation-induced emission (AIE) processed in a series of different TPA-based dyes in THF/water binary solvent systems [104]. The authors investigated the photophysical properties of the dyes solutions, aqueous aggregate suspensions, films and crystals. Crystallographic experiments were especially helpful in revealing some important trends. The results demonstrated that in general, formation of smaller and more uniform nanoaggregates favor more efficient emission. Close interactions such as π-π stacking favored the formation of excimers and had negative effects on fluorescence, whereas C-H…

π, C-H…N, CH…O and several other intra- and intermolecular interactions restrict the intramolecular motions and prevent the nonradiative processes. Overall it was demonstrated that even small structural changes in dye molecules can have a sensible effect on their molecular packing and thus photophysical properties of their aggregates.

Studies of various derivatives of perylene diimide (PDI) loaded into the polymeric PLGA nanoparticles also evidence for potentially negative effects of aggregation not only on the emission intensity, but also on photostability of the dye inside the nanomaterial [105]. The authors showed that a more substituted derivative, having bulky hydrophobic moieties in both imide and bay regions, showed almost no aggregation inside the polymer and possessed exceptionally high quantum yield and photostability. Side chains that regulate and alter the self-assembly of oligomers and polymers are also among the influencing factors that affect the nanoparticles photophysical properties. A study of a series of fluorene co-oligomers with naphthalene and benzothiadiazole substituted with hydrophobic alkyl and hydrophilic PEG side chains revealed that oligomers containing nonpolar chains formed smaller and more stable nanoparticles that generally had higher quantum yields of fluorescence [106]. The authors make an interesting observation that the emission efficacy can be affected by the interparticle material exchange, as more polar PEG-substituted nanoparticles showed lower stability and more intensive dynamics.

As the properties of the small molecule components can often translate to the characteristics of the supramolecular constructs, it is interesting to discuss another strategy that was recently reported for flavylium polymethine fluorophores [107]. By introducing conjugated heterocycles with dimethylamino electron donor groups to the sides of the polymethine chain, and a cyclohexene ring in the chain to reduce intramolecular motions, it was possible to achieve remarkable brightness and stability in the NIR and short wavelength infrared regions.

4.3. Size and Colloidal Stability

As part of the reprecipitation method, the compound's solution in a "good" solvent is poured into a larger volume of a "bad" solvent, where the compound is nearly insoluble. This leads to rapid association of the hydrophobic or amphiphilic molecules that tend to decrease their overall surface area. It is intuitive to assume that the higher initial concentration of the compound is, the faster the nucleation and growth processes will proceed on the early stages, which will lead to larger nanoaggregates, as was observed in particular by Breton *et al.* [77] as well as in many other reports. Lower concentrations of the injected solutions can also lead to better monodispersity of the resulting nanoaggregates [108]. The authors also evidence that introducing of the alkyl hydrophobic moieties to the dye molecules improves monodispersity and colloidal stability of the aggregates.

Oftentimes the nanoprecipitation is performed in combination with sonication, which arguably improves the dispersity of the obtained nanoparticles. Size control can be also achieved by sonication at different regimes or without the latter, as illustrated using TPE-based dye loaded into polymeric phosphoethanolamine-modified PEG nanoparticles using coprecipitation method [109]. Nanoparticles of various sizes were successfully obtained using the polymer stock solution of different concentrations, as well as sonication at various

power output and different time. The obtained nanoparticles were used to test the integrity of blood-brain barrier *in vivo*. Polymers are often used to improve solubility and stability of nanoaggregates. Using charged polymers for encapsulation of ionic aggregates allows to effectively control the size of nanoparticles obtained using the co-precipitation method [110]. Introducing just a few charged side- or end-groups, bearing either a negative or a positive charge, onto the polymer backbone can significantly decrease the nanoparticle size, and also plays the role in controlling the particle's zeta-potential. Further decrease of the particles sizes can be achieved by decreasing the concentration of the polymer solution used for nanoprecipitation. Similarly, variation in anion concentration, as well as concentration of the stabilizing neutral polymer during ion-association synthesis is reported to allow controlling the size of obtained carbocyanine-based nanoaggregates [111]. The size of obtained nanoaggregates also affects their spectral properties.

A classic example of controlling the size of the nanoparticles was described by Zhang *et al.* [112]. By introducing the hydrophobic and hydrophilic substituents of various sizes to the imide region of PDI, the curvature of the self-assembled micellar nanoparticles was gradually changed. This allowed to obtain a variety of co-assembled nanoparticles of different sizes. Similarly, co-assembly of two different organic fluorescent oligomers allowed controlling not only the sizes, but also surface charge - and thus cellular uptake - of the nanoparticles [113].

Both nature and concentration of the stabilizing surfactant can play a significant role in the self-assembly process, and thus in determining the size and stability of the nanoparticles [114]. It was shown that using anionic and cationic surfactants, or no surfactant at all, leads to obtaining the nanoparticles of different size and spectral properties. The work is also noteworthy for the example of fast solventless dye synthesis via Schiff condensation.

Nanoparticle size variation can be observed when polymers of different molecular weight are used for preparation. Nature and quantity of hydrophobic side chains also affect the size of nanoparticles prepared from amphiphilic polymers, such as hyaluronic acid modified with 5-β-cholanamide or pyrenebutanamide fragments (Fig. 8) [48]. The effects of nature of the hydrophobic side chains were studied in detail using a combination of computational and experimental methods [115]. In both cases the increasing hydrophobicity of the side fragment and use of shorter polymer chains usually led to smaller nanoparticles.

Properties of fluorescent nanomaterials are mostly determined by the properties of respective components, although their combination can sometimes lead to emergence of features that are otherwise impossible to obtain (Fig. 9). Tuning spectral properties, as well as brightness and stability of organic nanoparticles is usually achieved through changing of these properties for the precursor organic dyes. However, using multicomponent systems, controlling the self-assembly process, intermolecular and interparticle interactions can give a certain degree of control over these properties at a supramolecular level. Most commonly used approaches to control the sizes and improve colloidal stability of various nanoparticles are based on conditions used to prepare the nanomaterials. Particularities of the components, meanwhile, can also play a significant role in preparation of colloidal systems with desired properties.

CONCLUSIONS AND OUTLOOK

A rich variety of organic fluorescent supramolecular systems for various sensing and imaging applications were described, following the hierarchy of their increasing complexity - from small-molecule noncovalent aggregates to co-assembled core-shell nanoparticles. This perspective was logically built around common traits and differences in design approaches to preparation and modification of nanomaterials on the way to targeted synthesis of materials with predefined spectral and colloidal properties. To maintain the integrity of such approach, several types of bioinspired fluorescent macromolecules and nanoarchitectures, such as fluorescent proteins or DNA origami-based nanomaterials, were left beyond the scope of this review.

Several distinct current trends can be noted in the field of fluorescent nanomaterials research. The choice of fluorophores used to create fluorescent nanomaterials, both solely based on small molecules and combined with polymers or inorganic matrices, narrows to several leading classes, with AIEgenic compounds being of primary interest. Development of new precursors is mostly focused on modification or combination of well-known motifs. However, steps are made to explore their core modifications. Fundamental knowledge gained about intra- and intermolecular interactions being primary factors determining nanomaterials properties are leading these efforts. Additional studies will also help researchers shedding light onto a multitude of questions that still remain unanswered, such as nature of emission (and its excitation wavelength dependence) in carbohydrate-derived fluorescent polymers or behavior of nanomaterials of different levels of complexity at the nano-biointerface.

Analysis of past achievements and current trends allows to conclude that in the coming future, substantial research will be focused on advancing the field of smart and stimuli-responsive nanomaterials involving imaging and sensing modalities. Theoretical methods will become able to predict properties and behavior of complex systems based on knowledge about their components with increasing reliability, thus giving more weight to the computer-assisted design of nanomaterials. Flow chemistry will see wider applications for preparation of complex supramolecular systems, well beyond simple metal and polymeric nanoparticles. Development of flow reactors with feedback control will allow simpler and faster synthesis of uniform nanomaterials with high reproducibility.

ACKNOWLEDGEMENTS

This work was supported in part by NIH grants R21 CA212500 and P30 CA036727, and the Nebraska Research Initiative.

REFERENCES

[1]. Mei J; Leung NLC; Kwok RTK; Lam JWY; Tang BZ Aggregation-Induced Emission: Together We Shine, United We Soar! Chem. Rev 2015, 115, 11718–11940. [PubMed: 26492387]

[2]. Klymchenko AS Emerging Field of Self-Assembled Fluorescent Organic Dye Nanoparticles. J. Nanosci. Lett 2013, 3: 21, 1–8.

[3]. Demchenko AP Nanoparticles and Nanocomposites for Fluorescence Sensing and Imaging. Methods Appl. Fluoresc 2013, 1, 22001.

[4]. Liu M; Gao P; Wan Q; Deng F; Wei Y; Zhang X Recent Advances and Future Prospects of Aggregation-Induced Emission Carbohydrate Polymers. Macromol. Rapid Commun 2017, 38, 1600575.

[5]. Elsabahy M; Heo GS; Lim S-M; Sun G; Wooley KL Polymeric Nanostructures for Imaging and Therapy. Chem. Rev 2015, 115, 10967–11011. [PubMed: 26463640]

[6]. Reisch A; Klymchenko AS Fluorescent Polymer Nanoparticles Based on Dyes: Seeking Brighter Tools for Bioimaging. Small 2016, 12, 1968–1992. [PubMed: 26901678]

[7]. Hill TK; Mohs AM Image-Guided Tumor Surgery: Will There Be a Role for Fluorescent Nanoparticles? Wiley Interdiscip. Rev. Nanomedicine Nanobiotechnology 2016, 8, 498–511. [PubMed: 26585556]

[8]. Chinen AB; Guan CM; Ferrer JR; Barnaby SN; Merkel TJ; Mirkin CA Nanoparticle Probes for the Detection of Cancer Biomarkers, Cells, and Tissues by Fluorescence. Chem. Rev 2015, 115, 10530–10574. [PubMed: 26313138]

[9]. Würthner F Perylene Bisimide Dyes as Versatile Building Blocks for Functional Supramolecular Architectures. Chem. Commun 2004, 1564–1579.

[10]. Würthner F; Saha-Möller CR; Fimmel B; Ogi S; Leowanawat P; Schmidt D Perylene Bisimide Dye Assemblies as Archetype Functional Supramolecular Materials. Chem. Rev 2016, 116, 962–1052. [PubMed: 26270260]

[11]. Panthi K; Adhikari RM; Kinstle TH Visible and near IR Emitting Organic Nanoparticles of Aromatic Fumaronitrile Core-Based Donor-acceptor Compounds. J. Photochem. Photobiol. A Chem 2010, 215, 179–184.

[12]. Palayangoda SS; Cai X; Adhikari RM; Neckers DC Carbazole-Based Donor−Acceptor Compounds: Highly Fluorescent Organic Nanoparticles. Org. Lett 2008, 10, 281–284. [PubMed: 18092792]

[13]. Ishi-i T; Kitahara I; Yamada S; Sanada Y; Sakurai K; Tanaka A; Hasebe N; Yoshihara T; Tobita S Amphiphilic Benzothiadiazole-triphenylamine-Based Aggregates That Emit Red Light in Water. Org. Biomol. Chem 2015, 13, 1818–1828. [PubMed: 25502800]

[14]. Parthasarathy V; Fery-Forgues S; Campioli E; Recher G; Terenziani F; Blanchard-Desce M Dipolar versus Octupolar Triphenylamine-Based Fluorescent Organic Nanoparticles as Brilliant One- and Two-Photon Emitters for (Bio)imaging. Small 2011, 7, 3219–3229. [PubMed: 21972222]

[15]. Zhao Z; Lam JWY; Tang BZ Tetraphenylethene: A Versatile AIE Building Block for the Construction of Efficient Luminescent Materials for Organic Light-Emitting Diodes. J. Mater. Chem 2012, 22, 23726.

[16]. Ooyama Y; Sugino M; EnoKi T; Yamamoto K; Tsunoji N; Ohshita J Aggregation-Induced Emission (AIE) Characteristic of Water-Soluble Tetraphenylethene (TPE) Bearing Four Sulfonate Salts. New J. Chem 2017, 41, 4747–4749.

[17]. Miladi K; Sfar S; Fessi H; Elaissari A Nanoprecipitation Process: From Particle Preparation to *In Vivo* Applications In Polymer Nanoparticles for Nanomedicines; Vauthier C; Ponchel G, Eds.; Springer International Publishing: Cham, 2016; pp. 17–53.

[18]. Noroozi M; Radiman S; Zakaria A Influence of Sonication on the Stability and Thermal Properties of Al 2 O 3 Nanofluids. J. Nanomater 2014, 2014, 1–10.

[19]. Pradhan S; Hedberg J; Blomberg E; Wold S; Odnevall Wallinder I Effect of Sonication on Particle Dispersion, Administered Dose and Metal Release of Non-Functionalized, Non-Inert Metal Nanoparticles. J. Nanoparticle Res 2016, 18, 285.

[20]. Tang F; Wang C; Wang J; Wang X; Li L Fluorescent Organic Nanoparticles with Enhanced Fluorescence by Self-Aggregation and Their Application to Cellular Imaging. ACS Appl. Mater. Interfaces 2014, 6, 18337–18343. [PubMed: 25275214]

[21]. Barman S; Mukhopadhyay SK; Behara KK; Dey S; Singh NDP 1-Acetylpyrene-Salicylic Acid: Photoresponsive Fluorescent Organic Nanoparticles for the Regulated Release of a Natural Antimicrobial Compound, Salicylic Acid. ACS Appl. Mater. Interfaces 2014, 6, 7045–7054. [PubMed: 24800888]

[22]. Su S-Y; Lin H-H; Chang C-C Dual Optical Responses of Phenothiazine Derivatives: Near-IR Chromophore and Water-Soluble Fluorescent Organic Nanoparticles. J. Mater. Chem 2010, 20, 8653.

[23]. Hong G; Antaris AL; Dai H Near-Infrared Fluorophores for Biomedical Imaging. Nat. Biomed. Eng 2017, 1, 10.

[24]. Zhang J; Chen R; Zhu Z; Adachi C; Zhang X; Lee C-S Highly Stable Near-Infrared Fluorescent Organic Nanoparticles with a Large Stokes Shift for Noninvasive Long-Term Cellular Imaging. ACS Appl. Mater. Interfaces 2015, 7, 26266–26274. [PubMed: 26558487]

[25]. Denk W Two-Photon Excitation in Functional Biological Imaging. J. Biomed. Opt 1996, 1, 296. [PubMed: 23014729]

[26]. Amro K; Daniel J; Clermont G; Bsaibess T; Pucheault M; Genin E; Vaultier M; Blanchard-Desce M A New Route towards Fluorescent Organic Nanoparticles with Red-Shifted Emission and Increased Colloidal Stability. Tetrahedron 2014, 70, 1903–1909.

[27]. D'Aléo A; Felouat A; Heresanu V; Ranguis A; Chaudanson D; Karapetyan A; Giorgi M; Fages F Two-Photon Excited Fluorescence of BF 2 Complexes of Curcumin Analogues: Toward NIR-to-NIR Fluorescent Organic Nanoparticles. J. Mater. Chem. C 2014, 2, 5208–5215.

[28]. Zhang W; Ren Y-Y; Zhang L-N; Fan X; Fan H; Wu Y; Zhang Y; Kuang G-C Borondifluoride β-Diketonate Complex as Fluorescent Organic Nanoparticles: Aggregation-Induced Emission for Cellular Imaging. RSC Adv. 2016, 6, 101937–101940.

[29]. Shulov I; Arntz Y; Mély Y; Pivovarenko VG; Klymchenko AS Non-Coordinating Anions Assemble Cyanine Amphiphiles into Ultra-Small Fluorescent Nanoparticles. Chem. Commun 2016, 52, 7962–7965.

[30]. Das S; Debnath T; Basu A; Ghosh D; Das AK; Baker GA; Patra A Efficient White-Light Generation from Ionically Self-Assembled Triply-Fluorescent Organic Nanoparticles. Chem. - A Eur. J 2016, 22, 8855–8863.

[31]. Bwambok DK; El-Zahab B; Challa SK; Li M; Chandler L; Baker G. a.; Warner IM. Near-Infrared Fluorescent NanoGUMBOS for Biomedical Imaging. ACS Nano 2009, 3, 3854–3860. [PubMed: 19928781]

[32]. Petkau K; Kaeser A; Fischer I; Brunsveld L; Schenning APHJ Pre- and Postfunctionalized Self-Assembled π-Conjugated Fluorescent Organic Nanoparticles for Dual Targeting. J. Am. Chem. Soc 2011, 133, 17063–17071. [PubMed: 21913650]

[33]. Zhang X; Zhang X; Yang B; Zhang Y; Wei Y A New Class of Red Fluorescent Organic Nanoparticles: Noncovalent Fabrication and Cell Imaging Applications. ACS Appl. Mater. Interfaces 2014, 6, 3600–3606. [PubMed: 24555855]

[34]. Zhang X; Zhang X; Yang B; Zhang Y; Wei Y Facile Preparation of Water Dispersible Red Fluorescent Organic Nanoparticles and Their Cell Imaging Applications. Tetrahedron 2014, 70, 3553–3559.

[35]. Luo M Facile Preparation of Water Dispersible Red Fluorescent Organic Nanoparticles for Cell Imaging. Bull. Korean Chem. Soc 2014, 35, 1732–1736.

[36]. Wang Z; Yong T-Y; Wan J; Li Z-H; Zhao H; Zhao Y; Gan L; Yang X-L; Xu H-B; Zhang C Temperature-Sensitive Fluorescent Organic Nanoparticles with Aggregation-Induced Emission for Long-Term Cellular Tracing. ACS Appl. Mater. Interfaces 2015, 7, 3420–3425. [PubMed: 25602511]

[37]. Long Z; Liu M; Jiang R; Wan Q; Mao L; Wan Y; Deng F; Zhang X; Wei Y Preparation of Water Soluble and Biocompatible AIE-Active Fluorescent Organic Nanoparticles via Multicomponent Reaction and Their Biological Imaging Capability. Chem. Eng. J 2017, 308, 527–534.

[38]. Long Z; Liu M; Mao L; Zeng G; Wan Q; Xu D; Deng F; Huang H; Zhang X; Wei Y Rapid Preparation of Branched and Degradable AIE-Active Fluorescent Organic Nanoparticles via Formation of Dynamic Phenyl Borate Bond. Colloids Surfaces B Biointerfaces 2017, 150, 114–120. [PubMed: 27907858]

[39]. Lv Q; Wang K; Xu D; Liu M; Wan Q; Huang H; Liang S; Zhang X; Wei Y Synthesis of Amphiphilic Hyperbranched AIE-Active Fluorescent Organic Nanoparticles and Their Application in Biological Application. Macromol. Biosci 2016, 16, 223–230. [PubMed: 26376342]

[40]. Long Z; Liu M; Jiang R; Zeng G; Wan Q; Huang H; Deng F; Wan Y; Zhang X; Wei Y Ultrasonic-Assisted Kabachnik-Fields Reaction for Rapid Fabrication of AIE-Active Fluorescent Organic Nanoparticles. Ultrason. Sonochem 2017, 35, 319–325. [PubMed: 27773771]

[41]. Moholkar VS; Choudhury HA; Singh S; Khanna S; Ranjan A; Chakma S; Bhasarkar J Physical and Chemical Mechanisms of Ultrasound in Biofuel Synthesis In Production of Biofuels and Chemicals with Ultrasound; Fang Z; Smith RL; Qi X, Eds.; Springer International Publishing, 2015; pp. 35–86.

[42]. Cella R; Stefani HA Ultrasonic Reactions In Green Techniques for Organic Synthesis and Medicinal Chemistry; John Wiley & Sons, Ltd: Chichester, UK, 2012; pp. 343–361.

[43]. Liu M; Zhang X; Yang B; Liu L; Deng F; Zhang X; Wei Y Polylysine Crosslinked AIE Dye Based Fluorescent Organic Nanoparticles for Biological Imaging Applications. Macromol. Biosci 2014, 14, 1260–1267. [PubMed: 24854875]

[44]. Zhang X; Zhang X; Yang B; Liu L; Deng F; Hui J; Liu M; Chen Y; Wei Y Glycosylated Aggregation Induced Emission Dye Based Fluorescent Organic Nanoparticles: Preparation and Bioimaging Applications. RSC Adv. 2014, 4, 24189.

[45]. Pelaz B; del Pino P; Maffre P; Hartmann R; Gallego M; Rivera-Fernández S; de la Fuente JM; Nienhaus GU; Parak WJ Surface Functionalization of Nanoparticles with Polyethylene Glycol: Effects on Protein Adsorption and Cellular Uptake. ACS Nano 2015, 9, 6996–7008. [PubMed: 26079146]

[46]. Uthaman S; Lee SJ; Cherukula K; Cho C-S; Park IK Polysaccharide-Coated Magnetic Nanoparticles for Imaging and Gene Therapy. Biomed Res. Int 2015, 2015, 959175. [PubMed: 26078971]

[47]. Hill TK; Abdulahad A; Kelkar SS; Marini FC; Long TE; Provenzale JM; Mohs AM Indocyanine Green-Loaded Nanoparticles for Image-Guided Tumor Surgery. Bioconjug. Chem 2015, 26, 294–303. [PubMed: 25565445]

[48]. Hill TK; Kelkar SS; Wojtynek NE; Souchek JJ; Payne WM; Stumpf K; Marini FC; Mohs AM Near Infrared Fluorescent Nanoparticles Derived from Hyaluronic Acid Improve Tumor Contrast for ImageGuided Surgery. Theranostics 2016, 6, 2314–2328. [PubMed: 27877237]

[49]. Kelkar SS; Hill TK; Marini FC; Mohs AM Near Infrared Fluorescent Nanoparticles Based on Hyaluronic Acid: Self-Assembly, Optical Properties, and Cell Interaction. Acta Biomater. 2016, 36, 112–121. [PubMed: 26995504]

[50]. Payne WM; Hill TK; Svechkarev D; Holmes MB; Sajja BR; Mohs AM Multimodal Imaging Nanoparticles Derived from Hyaluronic Acid for Integrated Preoperative and Intraoperative Cancer Imaging. Contrast Media Mol. Imaging 2017, 2017, 1–14.

[51]. Tao Z; Hong G; Shinji C; Chen C; Diao S; Antaris AL; Zhang B; Zou Y; Dai H Biological Imaging Using Nanoparticles of Small Organic Molecules with Fluorescence Emission at Wavelengths Longer than 1000 Nm. Angew. Chemie Int. Ed 2013, 52, 13002–13006.

[52]. Dang X; Gu L; Qi J; Correa S; Zhang G; Belcher AM; Hammond PT Layer-by-Layer Assembled Fluorescent Probes in the Second near-Infrared Window for Systemic Delivery and Detection of Ovarian Cancer. Proc. Natl. Acad. Sci 2016, 113, 5179–5184. [PubMed: 27114520]

[53]. Wu I-C; Yu J; Ye F; Rong Y; Gallina ME; Fujimoto BS; Zhang Y; Chan Y-H; Sun W; Zhou X-H; et al. Squaraine-Based Polymer Dots with Narrow, Bright Near-Infrared Fluorescence for Biological Applications. J. Am. Chem. Soc 2015, 137, 173–178. [PubMed: 25494172]

[54]. Hong G; Zou Y; Antaris AL; Diao S; Wu D; Cheng K; Zhang X; Chen C; Liu B; He Y; et al. Ultrafast Fluorescence Imaging *in Vivo* with Conjugated Polymer Fluorophores in the Second near-Infrared Window. Nat. Commun 2014, 5, 4206. [PubMed: 24947309]

[55]. Liu M; Zhang X; Yang B; Li Z; Deng F; Yang Y; Zhang X; Wei Y Fluorescent Nanoparticles from Starch: Facile Preparation, Tunable Luminescence and Bioimaging. Carbohydr. Polym 2015, 121, 49–55. [PubMed: 25659670]

[56]. Ma C; Zhang X; Yang L; Wu Y; Liu H; Zhang X; Wei Y Preparation of Fluorescent Organic Nanoparticles from Polyethylenimine and Sucrose for Cell Imaging. Mater. Sci. Eng. C 2016, 68, 37–42.

[57]. Shi Y; Jiang R; Liu M; Fu L; Zeng G; Wan Q; Mao L; Deng F; Zhang X; Wei Y Facile Synthesis of Polymeric Fluorescent Organic Nanoparticles Based on the Self-Polymerization of Dopamine for Biological Imaging. Mater. Sci. Eng. C 2017, 77, 972–977.

[58]. Wu S-Y; Debele T; Kao Y-C; Tsai H-C Synthesis and Characterization of Dual-Sensitive Fluorescent Nanogels for Enhancing Drug Delivery and Tracking Intracellular Drug Delivery. Int. J. Mol. Sci 2017, 18, 1090.

[59]. Aslan K; Gryczynski I; Malicka J; Matveeva E; Lakowicz JR; Geddes CD Metal-Enhanced Fluorescence: An Emerging Tool in Biotechnology. Curr. Opin. Biotechnol 2005, 16, 55–62. [PubMed: 15722016]

[60]. Bharti C; Gulati N; Nagaich U; Pal A Mesoporous Silica Nanoparticles in Target Drug Delivery System: A Review. Int. J. Pharm. Investig 2015, 5, 124.

[61]. Wang Y; Zhao Q; Han N; Bai L; Li J; Liu J; Che E; Hu L; Zhang Q; Jiang T; et al. Mesoporous Silica Nanoparticles in Drug Delivery and Biomedical Applications. Nanomedicine Nanotechnology, Biol. Med 2015, 11, 313–327.

[62]. Sun L; Liu T; Li H; Yang L; Meng L; Lu Q; Long J Fluorescent and Cross-Linked Organic-Inorganic Hybrid Nanoshells for Monitoring Drug Delivery. ACS Appl. Mater. Interfaces 2015, 7, 4990–4997. [PubMed: 25651861]

[63]. Oltolina F; Gregoletto L; Colangelo D; Gómez-Morales J; Delgado-López JM; Prat M Monoclonal AntibodyTargeted Fluorescein-5-Isothiocyanate-Labeled Biomimetic Nanoapatites: A Promising Fluorescent Probe for Imaging Applications. Langmuir 2015, 31, 1766–1775. [PubMed: 25602940]

[64]. Chen M; Yin M Design and Development of Fluorescent Nanostructures for Bioimaging. Prog. Polym. Sci 2014, 39, 365–395.

[65]. Smith BR; Gambhir SS Nanomaterials for *In Vivo* Imaging. Chem. Rev 2017, 117, 901–986. [PubMed: 28045253]

[66]. Linot C; Poly J; Boucard J; Pouliquen D; Nedellec S; Hulin P; Marec N; Arosio P; Lascialfari A; Guerrini A; et al. PEGylated Anionic Magnetofluorescent Nanoassemblies: Impact of Their Interface Structure on Magnetic Resonance Imaging Contrast and Cellular Uptake. ACS Appl. Mater. Interfaces 2017, 9, 14242–14257. [PubMed: 28379690]

[67]. Faucon A; Benhelli-Mokrani H; Fleury F; Dubreil L; Hulin P; Nedellec S; Doussineau T; Antoine R; Orlando T; Lascialfari A; et al. Tuning the Architectural Integrity of High-Performance Magneto-Fluorescent Core-Shell Nanoassemblies in Cancer Cells. J. Colloid Interface Sci 2016, 479, 139–149. [PubMed: 27388127]

[68]. Reddy ER; Banote RK; Chatti K; Kulkarni P; Rajadurai MS Selective Multicolour Imaging of Zebrafish Muscle Fibres by Using Fluorescent Organic Nanoparticles. ChemBioChem 2012, 13, 1889–1894. [PubMed: 22887835]

[69]. Jana A; Saha B; Banerjee DR; Ghosh SK; Nguyen KT; Ma X; Qu Q; Zhao Y; Singh ND P. Photocontrolled Nuclear-Targeted Drug Delivery by Single Component Photoresponsive Fluorescent Organic Nanoparticles of Acridin-9-Methanol. Bioconjug. Chem 2013, 24, 1828–1839. [PubMed: 24195782]

[70]. Pramanik M; Chatterjee N; Das S; Saha K. Das; Bhaumik A. Anthracene-Bisphosphonate Based Novel Fluorescent Organic Nanoparticles Explored as Apoptosis Inducers of Cancer Cells. Chem. Commun 2013, 49, 9461.

[71]. Yang Y; Wang X; Cui Q; Cao Q; Li L Self-Assembly of Fluorescent Organic Nanoparticles for Iron(III) Sensing and Cellular Imaging. ACS Appl. Mater. Interfaces 2016, 8, 7440–7448. [PubMed: 26950776]

[72]. Huerta-Aguilar CA; Raj P; Thangarasu P; Singh N Fluorescent Organic Nanoparticles (FONs) for Selective Recognition of Al 3+: Application to Bio-Imaging for Bacterial Sample. RSC Adv. 2016, 6, 37944–37952.

[73]. Huerta-Aguilar CA; Pandiyan T; Raj P; Singh N; Zanella R Fluorescent Organic Nanoparticles (FONs) for the Selective Recognition of Zn 2+: Applications to MultiVitamin Formulations in Aqueous Medium. Sensors Actuators B Chem. 2016, 223, 59–67.

[74]. Kaur A; Raj T; Kaur S; Singh N; Kaur N Fluorescent Organic Nanoparticles of Dihydropyrimidone Derivatives for Selective Recognition of Iodide Using a Displacement Assay:

Application of the Sensors in Water and Biological Fluids. Org. Biomol. Chem 2015, 13, 1204–1212. [PubMed: 25428514]

[75]. You C-C; Miranda OR; Gider B; Ghosh PS; Kim I-B; Erdogan B; Krovi SA; Bunz UHF; Rotello VM Detection and Identification of Proteins Using Nanoparticle-Fluorescent Polymer “chemical Nose’ Sensors. Nat. Nanotechnol 2007, 2, 318–323. [PubMed: 18654291]

[76]. Faucon A; Benhelli-Mokrani H; Córdova L. A.w.; Brulin B; Heymann D; Hulin P; Nedellec S; Ishow E. Are Fluorescent Organic Nanoparticles Relevant Tools for Tracking Cancer Cells or Macrophages? Adv. Healthc. Mater 2015, 4, 2727–2734. [PubMed: 26548458]

[77]. Breton M; Prével G; Audibert J-F; Pansu R; Tauc P; Pioufle B.Le; Français O; Fresnais J; Berret J-F; Ishow E. Solvatochromic Dissociation of Non-Covalent Fluorescent Organic Nanoparticles upon Cell Internalization. Phys. Chem. Chem. Phys 2011, 13, 13268. [PubMed: 21701730]

[78]. Milosevic AM; Rodriguez-Lorenzo L; Balog S; Monnier CA; Petri-Fink A; Rothen-Rutishauser B Assessing the Stability of Fluorescently Encoded Nanoparticles in Lysosomes by Using Complementary Methods. Angew. Chemie Int. Ed 2017, 1–6.

[79]. Chopra S; Singh J; Kaur H; Singh N; Kaur N Estimation of Biogenic Amines and Biothiols by Metal Complex of Fluorescent Organic Nanoparticles Acting as Single Receptor Multi-Analyte Sensor in Aqueous Medium. Sensors Actuators B Chem 2015, 220, 295–301.

[80]. Bhardwaj VK; Sharma H; Singh N Ratiometric Fluorescent Probe for Biothiol in Aqueous Medium with Fluorescent Organic Nanoparticles. Talanta 2014, 129, 198202.

[81]. Svechkarev DA; Bukatich IV; Doroshenko AO New 1,3,5-Triphenyl-2-Pyrazoline-Containing 3-Hydroxychromones as Highly Solvatofluorochromic Ratiometric Polarity Probes. J. Photochem. Photobiol. A Chem 2008, 200, 426–431.

[82]. Svechkarev DA; Baumer VN; Syzova ZA; Doroshenko AO New Benzimidazolic 3Hydroxychromone Derivative with Two Alternative Mechanisms of the Excited State Intramolecular Proton Transfer Reaction. J. Mol. Struct 2008, 882, 63–69.

[83]. Chen Q; Jia C; Zhang Y; Du W; Wang Y; Huang Y; Yang Q; Zhang Q A Novel Fluorophore Based on the Coupling of AIE and ESIPT Mechanisms and Its Application in Biothiol Imaging. J. Mater. Chem. B 2017, 5, 7736–7742.

[84]. Yin C-X; Xiong K-M; Huo F-J; Salamanca JC; Strongin RM Fluorescent Probes with Multiple Binding Sites for the Discrimination of Cys, Hcy, and GSH. Angew. Chemie Int. Ed 2017, 2–13.

[85]. Petrizza L; Collot M; Richert L; Mely Y; Prodi L; Klymchenko AS Dye-Doped Silica Nanoparticle Probes for Fluorescence Lifetime Imaging of Reductive Environments in Living Cells. RSC Adv. 2016, 6, 104164104172.

[86]. Mahajan PG; Kolekar GB; Patil SR Recognition of D-Penicillamine Using Schiff Base Centered Fluorescent Organic Nanoparticles and Application to Medicine Analysis. J. Fluoresc 2017, 27, 829–839. [PubMed: 28091784]

[87]. Ding L; Qin Z; Xiang C; Zhou G Novel Fluorescent Organic Nanoparticles as a Label-Free Biosensor for Dopamine in Serum. J. Mater. Chem. B 2017, 5, 2750–2756.

[88]. Hu J; Liu G; Wang C; Liu T; Zhang G; Liu S Spatiotemporal Monitoring Endocytic and Cytosolic pH Gradients with Endosomal Escaping pH-Responsive Micellar Nanocarriers. Biomacromolecules 2014, 15, 4293–4301. [PubMed: 25317967]

[89]. Kaur G; Raj T; Kaur N; Singh N Pyrimidine-Based Functional Fluorescent Organic Nanoparticle Probe for Detection of Pseudomonas Aeruginosa. Org. Biomol. Chem 2015, 13, 4673–4679. [PubMed: 25790762]

[90]. Jana A; Devi KSP; Maiti TK; Singh NDP Perylene-3-Ylmethanol: Fluorescent Organic Nanoparticles as a Single-Component Photoresponsive Nanocarrier with Real-Time Monitoring of Anticancer Drug Release. J. Am. Chem. Soc 2012, 134, 7656–7659. [PubMed: 22519548]

[91]. Gangopadhyay M; Singh T; Behara KK; Karwa S; Ghosh SK; Singh NDP Coumarin-Containing-StarShaped 4-Arm-Polyethylene Glycol: Targeted Fluorescent Organic Nanoparticles for Dual Treatment of Photodynamic Therapy and Chemotherapy. Photochem. Photobiol. Sci 2015, 14, 1329–1336. [PubMed: 26066468]

[92]. Chang C-C; Hsieh M-C; Lin J-C; Chang T-C Selective Photodynamic Therapy Based on Aggregation-Induced Emission Enhancement of Fluorescent Organic Nanoparticles. Biomaterials 2012, 33, 897–906. [PubMed: 22024361]

[93]. Han H-H; Wang C-Z; Zang Y; Li J; James TD; He X-P Supramolecular Core-glycoshell Polythiophene Nanodots for Targeted Imaging and Photodynamic Therapy. Chem. Commun 2017, 53, 9793–9796.

[94]. Ng KK; Zheng G Molecular Interactions in Organic Nanoparticles for Phototheranostic Applications. Chem. Rev 2015, 115, 11012–11042. [PubMed: 26244706]

[95]. Wu X; Zhu W Stability Enhancement of Fluorophores for Lighting up Practical Application in Bioimaging. Chem. Soc. Rev 2015, 44, 4179–4184. [PubMed: 25175934]

[96]. Genin E; Gao Z; Varela JA; Daniel J; Bsaibess T; Gosse I; Groc L; Cognet L; Blanchard-Desce M "Hyper-Bright" Near-Infrared Emitting Fluorescent Organic Nanoparticles for Single Particle Tracking. Adv. Mater 2014, 26, 2258–2261. [PubMed: 24497445]

[97]. Grimm JB; Muthusamy AK; Liang Y; Brown TA; Lemon WC; Patel R; Lu R; Macklin JJ; Keller PJ; Ji N; et al. A General Method to Fine-Tune Fluorophores for Live-Cell and in Vivo Imaging. Nat. Methods 2017, 14, 987–994. [PubMed: 28869757]

[98]. Xu Z; Liao Q; Shi X; Li H; Zhang H; Fu H FullColor Tunable Organic Nanoparticles with FRET-Assisted Enhanced Two-Photon Excited Fluorescence for BioImaging. J. Mater. Chem. B 2013, 1, 6035.

[99]. Zhang T; Xu H; Wang H; Zhu J; Zhai Y; Bai X; Dong B; Song H Green Fluorescent Organic Nanoparticles Based on Carbon Dots and Self-Polymerized Dopamine for Cell Imaging. RSC Adv. 2017, 7, 28987–28993.

[100]. Varghese B; Al-Busafi SN; Suliman FO; Al-Kindy SMZ Unveiling a Versatile Heterocycle: Pyrazoline - a Review. RSC Adv. 2017, 7, 46999–47016.

[101]. Das S; Bwambok D; El-Zahab B; Monk J; de Rooy SL; Challa S; Li M; Hung FR; Baker GA; Warner IM Nontemplated Approach to Tuning the Spectral Properties of Cyanine-Based Fluorescent NanoGUMBOS. Langmuir 2010, 26, 12867–12876. [PubMed: 20583774]

[102]. Handke M; Adachi T; Hu C; Ward MD Encapsulation of Isolated Luminophores within Supramolecular Cages. Angew. Chemie Int. Ed 2017, 1–5.

[103]. Shulov I; Oncul S; Reisch A; Arntz Y; Collot M; Mely Y; Klymchenko AS Fluorinated CounterionEnhanced Emission of Rhodamine Aggregates: Ultrabright Nanoparticles for Bioimaging and Light-Harvesting. Nanoscale 2015, 7, 18198–18210. [PubMed: 26482443]

[104]. Yang M; Xu D; Xi W; Wang L; Zheng J; Huang J; Zhang J; Zhou H; Wu J; Tian Y Aggregation-Induced Fluorescence Behavior of Triphenylamine-Based Schiff Bases: The Combined Effect of Multiple Forces. J. Org. Chem 2013, 78, 10344–10359. [PubMed: 24050697]

[105]. Trofymchuk K; Reisch A; Shulov I; Mély Y; Klymchenko AS Tuning the Color and Photostability of Perylene Diimides inside Polymer Nanoparticles: Towards Biodegradable Substitutes of Quantum Dots. Nanoscale 2014, 6, 12934–12942. [PubMed: 25233438]

[106]. Kaeser A; Fischer I; Abbel R; Besenius P; Dasgupta D; Gillisen M. a J.; Portale G; Stevens AL; Herz LM; Schenning APHJ Side Chains Control Dynamics and Self-Sorting in Fluorescent Organic Nanoparticles. ACS Nano 2013, 7, 408–416. [PubMed: 23256849]

[107]. Cosco ED; Caram JR; Bruns OT; Franke D; Day RA; Farr EP; Bawendi MG; Sletten EM Flavylium Polymethine Fluorophores for Near- and Shortwave Infrared Imaging. Angew. Chemie Int. Ed 2017, 56, 13126–13129.

[108]. Svechkarev D; Kyrychenko A; Payne WM; Mohs AM Development of Colloidally Stable Carbazole-Based Fluorescent Nanoaggregates. J. Photochem. Photobiol. A Chem 2018, 352, 55–64. [PubMed: 29430162]

[109]. Cai X; Bandla A; Mao D; Feng G; Qin W; Liao LD; Thakor N; Tang BZ; Liu B Biocompatible Red Fluorescent Organic Nanoparticles with Tunable Size and Aggregation-Induced Emission for Evaluation of Blood-Brain Barrier Damage. Adv. Mater 2016, 28, 8760–8765. [PubMed: 27511643]

[110]. Reisch A; Runser A; Arntz Y; Mély Y; Klymchenko AS Charge-Controlled Nanoprecipitation as a Modular Approach to Ultrasmall Polymer Nanocarriers: Making Bright and Stable Nanoparticles. ACS Nano 2015, 9, 5104–5116. [PubMed: 25894117]

[111]. Enseki T; Yao H Controlled Formation of Fluorescent Organic Nanoparticles of Carbocyanine Dye via Ion-Association Approach. Chem. Lett 2012, 41, 1119–1121.

[112]. Zhang X; Chen Z; Würthner F Morphology Control of Fluorescent Nanoaggregates by Co-Self-Assembly of Wedge- and Dumbbell-Shaped Amphiphilic Perylene Bisimides. J. Am. Chem. Soc 2007, 129, 4886–4887. [PubMed: 17402739]

[113]. Fischer I; Petkau-Milroy K; Dorland YL; Schenning APHJ; Brunsveld L Self-Assembled Fluorescent Organic Nanoparticles for Live-Cell Imaging. Chem. - A Eur. J 2013, 19, 16646–16650.

[114]. Omer KM; Mohammad SJ; Raheem SJ Solventless Synthesis of a Schiff Base That Forms Highly Fluorescent Organic Nanoparticles Exhibiting Aggregation-Induced Emission in Aqueous Media. J. Exp. Nanosci 2016, 11, 1184–1192.

[115]. Payne WM; Svechkarev D; Kyrychenko A; Mohs AM The Role of Hydrophobic Modification on Hyaluronic Acid Dynamics and Self-Assembly. Carbohydr. Polym 2018, 182, 132–141. [PubMed: 29279107]

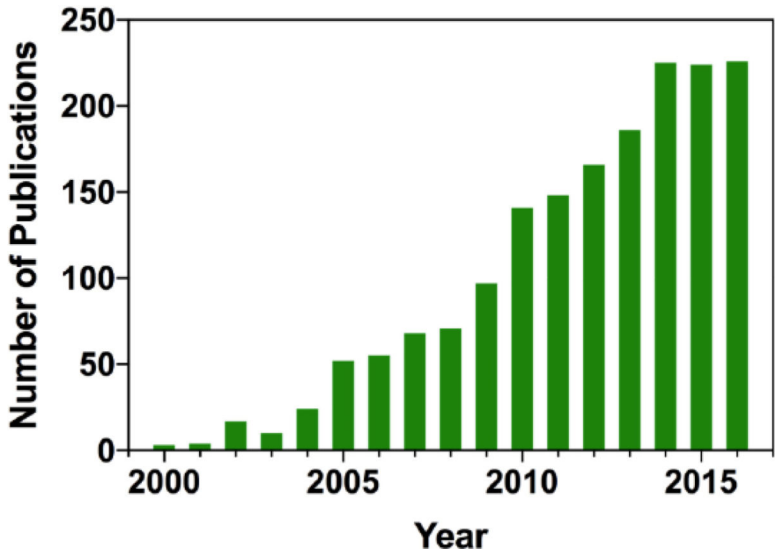

Fig. (1).

Number of publications mentioning fluorescent organic nanoparticles by year (based on data obtained from SciFinder).

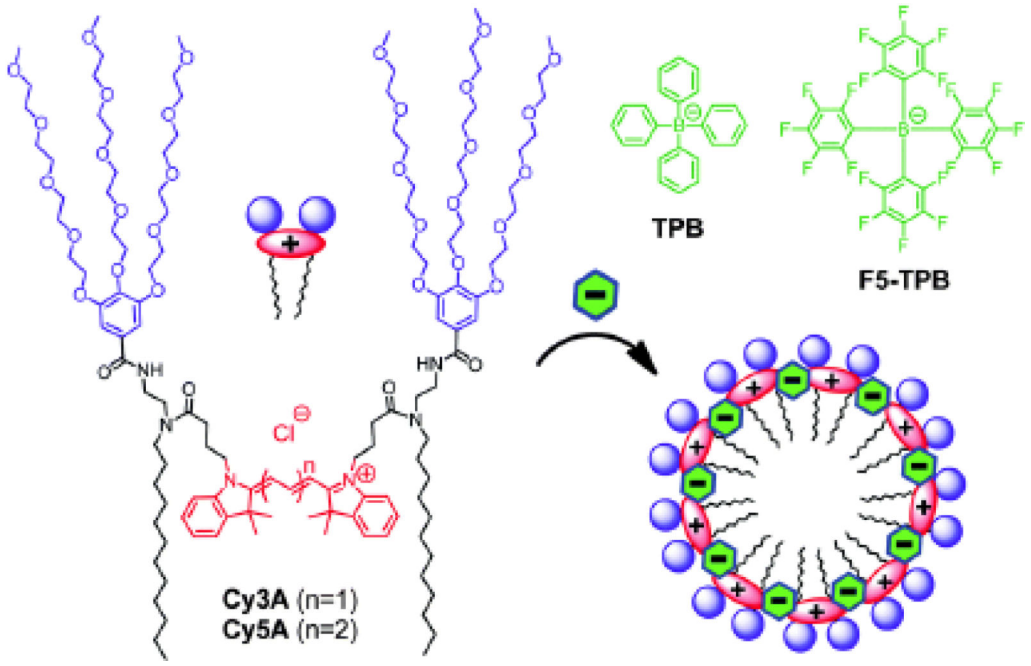

Fig. (2).

Cyanine dyes and their expected assembly into micelles in the presence of non-coordinating ions (reproduced with permission from Shulov *et al.* [29] Copyright © The Royal Society of Chemistry, 2016).

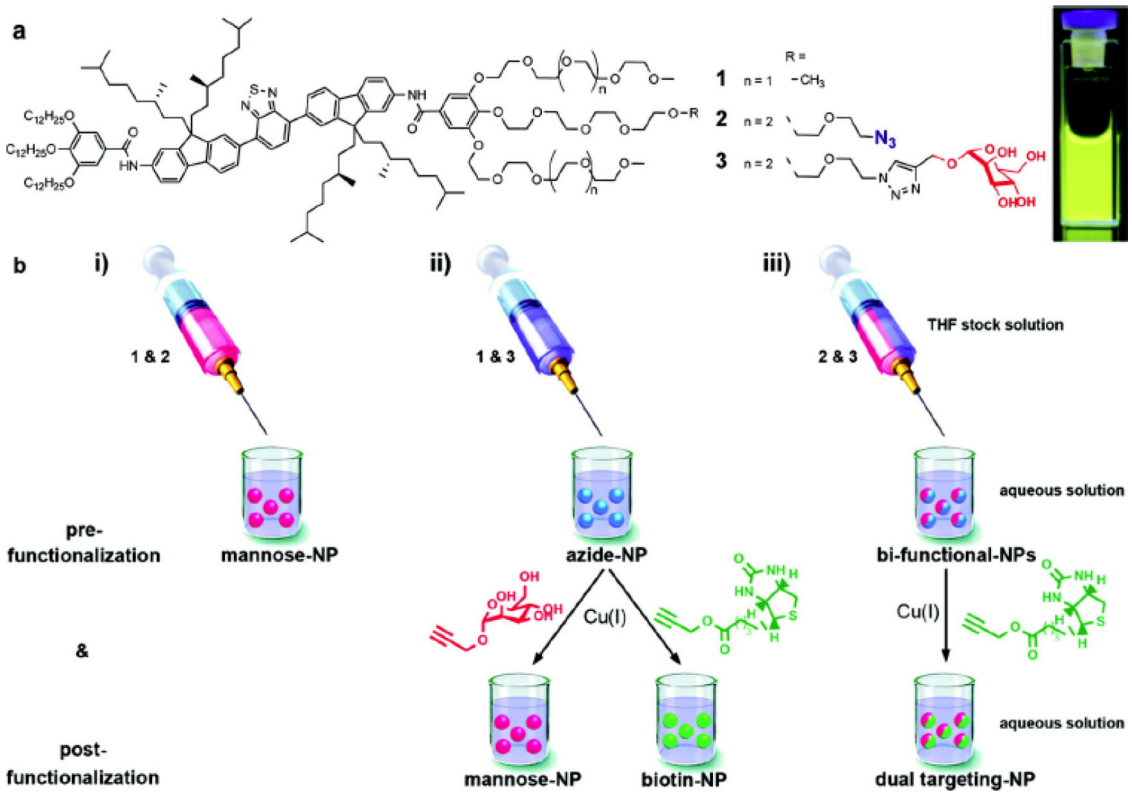

Fig. (3).

(a) Chemical structures of amphiphiles and a photograph of a 0.3 μM nanoparticle solution under UV light (360 nm). (b)(i) Generation of nanoparticles prefunctionalized with mannose using mixtures of **1** and **2**. (ii) Generation of nanoparticles prefunctionalized with azides using mixtures of **1** and **3** and their subsequent postfunctionalization via copper catalyzed azide-alkyne cycloaddition with alkyne derivatives of either mannose or biotin. (iii) Generation of bifunctional nanoparticles containing azides and mannose using mixtures of **2** and **3** and their subsequent postfunctionalization via copper catalyzed azide-alkyne cycloaddition with alkyne derived biotin yielding dual targeting mannose and biotin labeled nanoparticles (reproduced with permission from Petkau *et al.* [32] Copyright © American Chemical Society, 2011).

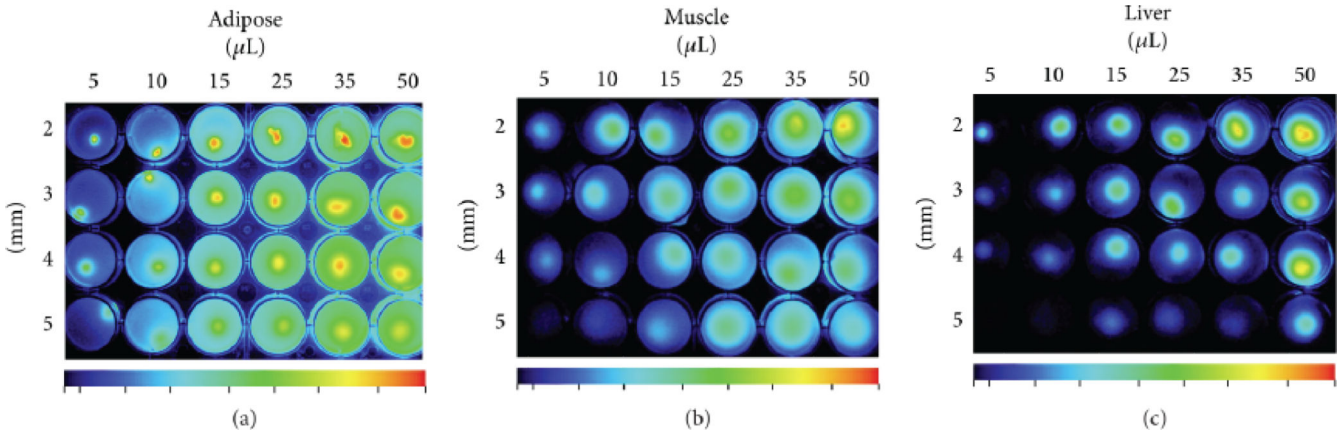

Fig. (4).

In vitro studies of depth detection and cellular uptake of self-assembled multimodal imaging nanoparticles. Fluorescence contrast in three different simulated tissue phantom models demonstrates viability as a contrast agent in a variety of tissue types, showing the contrast fluorescence image of tumor-like inclusions embedded into (a) adipose, (b) muscle and (c) liver tissue phantoms (adapted from Payne *et al.* [50] Copyright © William M. Payne *et al.*, 2017).

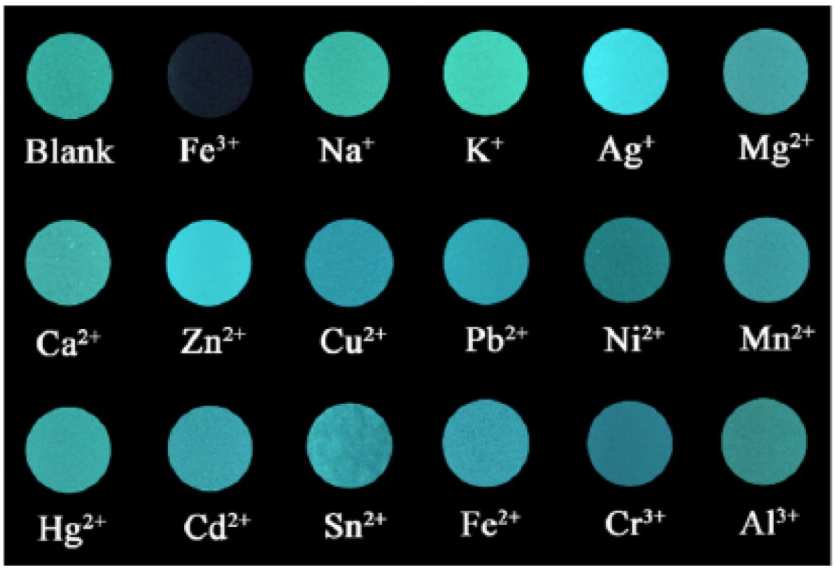

Fig. (5).

Fluorescence changes from the photographs of TPE-BIMEG/ATP dispersions in the presence of various metal ions (1 mM) under a hand-held UV lamp illumination at 365 nm (reproduced with permission from Yang *et al.* [71]. Copyright © American Chemical Society, 2016).

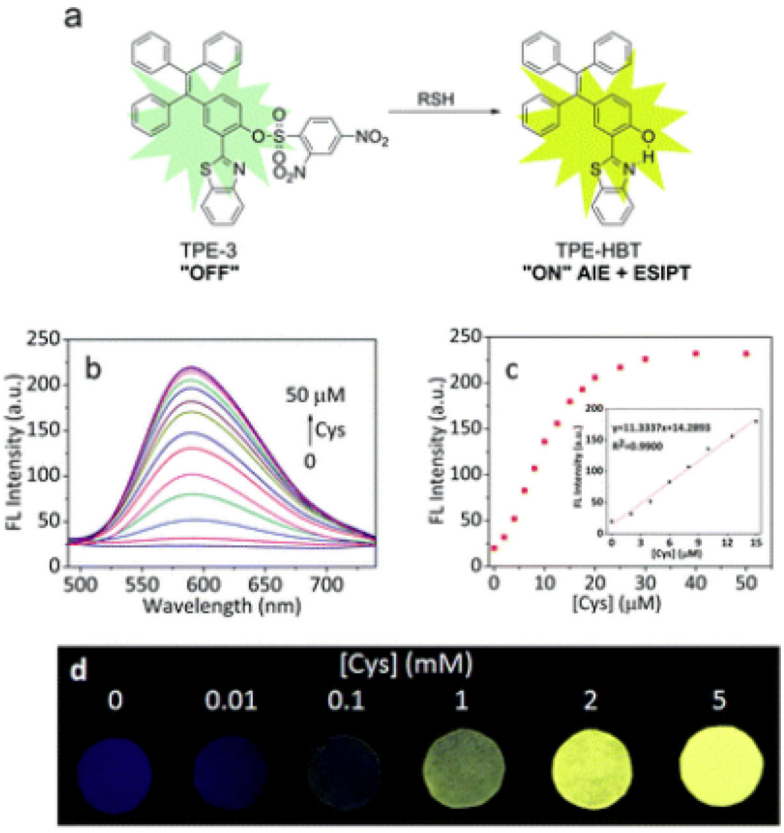

Fig. (6).

(a) Proposed sensing mechanism for TPE-3 and biothiols. (b) Fluorescence spectra of TPE-3 (10 μM) upon addition of Cys (0–50 μM) in PBS buffer (10 mM, pH = 7.4, containing 45% DMSO). (c) Fluorescence response of TPE-3 at 589 nm to Cys concentration (0 – 50 μM). Inset: linear range for Cys detection. Spectra were recorded after incubation with different concentrations of Cys for 15 min, λ_{ex} = 370 nm. (d) Fluorescent photographs of TPE-3 deposited on test papers after immersed into buffer solutions (10 mM, pH = 7.4) with different concentrations of Cys under a UV lamp (365 nm) (reproduced with permission from Chen *et al.* [83] Copyright © The Royal Society of Chemistry, 2017).

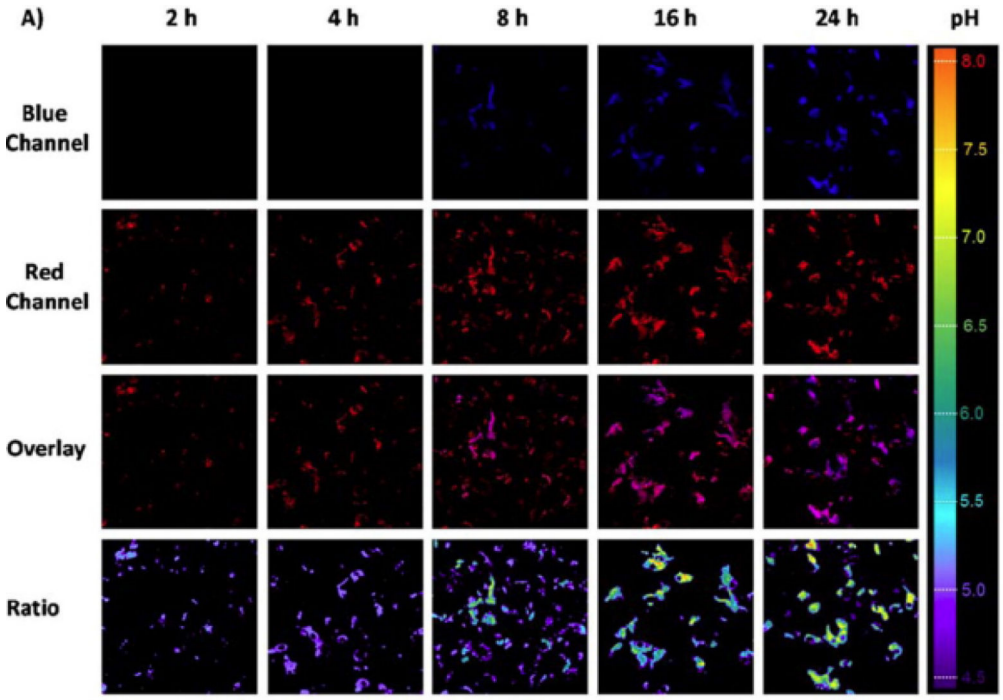

Fig. (7).

Incubation duration-dependent confocal laser scanning microscopy images of live HepG2 cells when culturing with BP6 copolymer at 37 °C (adapted with permission from Hu *et al.* [88] Copyright © American Chemical Society, 2014).

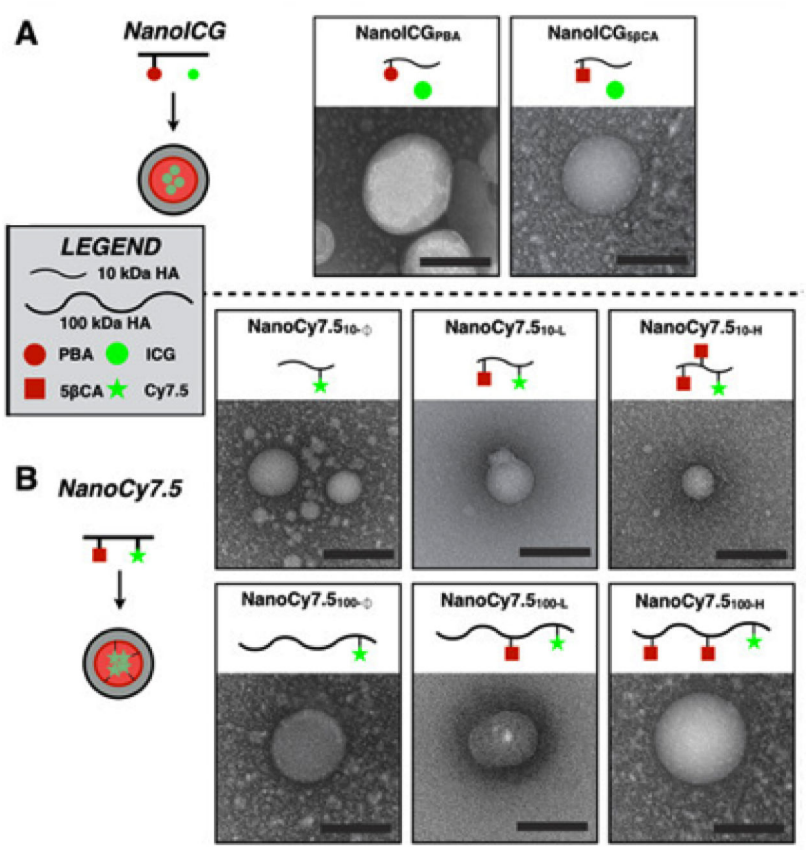

Fig. (8).

Transmission electron microscopy images of HA-based NPs that were derived from 10 kDa or 100 kDa HA, using either PBA or 5βCA as hydrophobic substituents to drive self-assembly (scale bars = 100 nm). The subscript “100” or “10” refers to 100 or 10 kDa HA, respectively. “H”, “L”, and “Ø” refer to high, low, or no hydrophobic ligand conjugation to HA. (adapted from Hill *et al.* [48] Copyright © Ivyspring International Publisher, 2016).

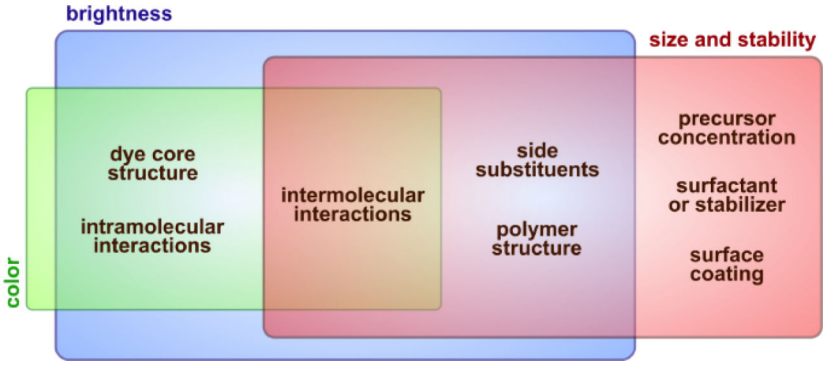

Fig. (9).

A broad spectrum of factors, internal and external, affect the properties of fluorescent nanomaterials. Selecting an optimal combination of intrinsic properties of the components and the preparation procedure is of great importance for obtaining the nanomaterial with desired properties.